

# An analysis of an extreme rainstorm caused by the interaction of the Tibetan Plateau vortex and the Southwest China vortex from an intensive observation

Xiaolong Cheng<sup>1,2</sup> · Yueqing Li<sup>1,2</sup> · Li Xu<sup>3</sup>

Received: 23 July 2015 / Accepted: 24 November 2015 / Published online: 11 December 2015  
© Springer-Verlag Wien 2015

**Abstract** A rainstorm caused by the coupling of the Tibetan Plateau vortex (TPV) and the Southwest China vortex (SWCV) in eastern Sichuan during 29 June–2 July 2013 is analyzed by using the conventional observed data and its time intensive observed data, the intensive observed data of SWCV scientific experiment during flood season. The results show that under the control of a large transverse trough in Eurasia region at mid-high latitude, the westerly flow in northern China leads TPV eastward movement. And SWCV moves northeastward. Finally, both of them merge to form a combined vortex (CBV) in Sichuan Basin resulting in heavy rainfall. The water vapor from both the Bay of Bengal and the South China Sea provides the sufficient humidity condition. The intensive observation clearly reveals the nascent states of TPV and SWCV, the movements and interactions, especially, the two vortices' merging process, and the effects of cold and warm advection, as well as the rainstorm. When the two vortices merge into CBV, cold tongue and warm flow meet and produce frontogenesis around the center of CBV. A frontogenetical area exists deeply from lower troposphere to upper troposphere with the south-positive and north-negative vertical structure, which is similar to front. The

positive PV evidently developed both in the range and in the intensity with the stronger center at upper level, and the positive PV center located at the front of CBV has indicative significance for the vortex's activities. And CBV has the same distributions of vorticity and temperature with SWCV and TPV, respectively. SWCV and TPV make different key contributions to the dynamic–thermodynamic property of CBV, but both of them have obvious influences on the divergence distribution of CBV. Furthermore, rainfall mainly distributes in the high areas of averaged temperature deviation gradient, and it is closely related to the joint influences of warm-moist air from the south and dry-cold air from the north. But, only using the conventional observed data, it is difficult to obtain the above useful understanding. So, augmenting intensive observation, improving scientific experiment, and focusing on fine study are much conducive for the meso-scale and small-scale weather systems such as SWCV and TPV, as well as its weather influences.

## 1 Introduction

The Tibetan Plateau vortex (TPV) is a low-pressure system, which appears at 500 hPa over the Qinghai-Tibetan Plateau (Lhasa Project Group 1981), and usually forms under the dynamic and thermodynamic effects of the Plateau (Zhang and Zhu 1988; Luo 1992). The horizontal scale of TPV is about 500 km and the vertical thickness of it is about 2–3 km (Ye and Gao 1979). TPV can be divided into cold and warm vortex by nature. The cold one typically originates in the southwestern Plateau or at the north side of the Plateau, usually is large and relatively deep, and mainly appears in winter half year with significant rainfall.

Responsible Editor: M. Kaplan.

✉ Yueqing Li  
yueqingli@163.com

- <sup>1</sup> Institute of Plateau Meteorology, China Meteorological Administration (CMA), Chengdu 610072, China
- <sup>2</sup> Heavy Rain and Drought-Flood Disasters in Plateau and Basin Key Laboratory of Sichuan Province, Chengdu 610072, China
- <sup>3</sup> Climate Prediction Center/NCEP/NOAA, 5830 University Research Court, Rm 3101, College Park, MD 20740, USA

The warm one basically originates in the central Plateau, the southern Plateau or Qaidam Basin in summer half year, being a shallow system with less movement, and has not significant precipitation in source regions. The previous researches show that the effects of terrain and sensible heat play an important role in the generation of TPV (Shen et al. 1986; Wang 1987; Wu and Chen 1985). The larger the difference between surface temperature and atmospheric temperature, the more it is beneficial for vortex development (Li and Liu 2006); however, latent heat plays a major role in TPV movement (Xiang et al. 2013). By numerical simulation, it had been found that the development of TPV in rainy season is due to the interaction of orographic effect, large-scale circulation, and convective cumulus latent heat release (Wang and Orlanski 1987; Wang 1987). Meanwhile, TPV usually develops and moves along the eastward, northeastward, and southeastward paths, causing rainstorm weather in the vast downstream area (Chen and Dell'osso 1984; Tao and Ding 1981).

Generated by the interaction of atmospheric circulation and special terrain of the Plateau, also being known as a closed meso-scale low, the Southwest China vortex (SWCV) originates at the middle or low troposphere such as at 700 or 850 hPa (Lu 1986; Luo and Wei 1985; Li 2007; Chen et al. 2007). SWCV is a shallow disturbance, exhibiting meso-scale cyclone characteristics, which is almost round and asymmetrical. The strong developed SWCV could extend up to 100 hPa, which is extraordinary deep (Chen et al. 1998). The humidity around it is very large, hardly existing wind shear (Wang et al. 1993). The temperature profile is nearly moist adiabatic. Moreover, latent heat release is important for the development of SWCV (Ying et al. 1988). In heavy rainfall, there frequently appears oblique  $\beta$  meso-scale vortex in the interior of SWCV with typical vertical structure of rainstorm (Gu et al. 2008). Under the background of saddle-pattern large-scale circulation, strong southwesterly flow could enter Sichuan Basin around the east side of the Tibetan Plateau, which forms a convergence zone in Sichuan Basin to benefit the development of SWCV due to the effects of terrain blocking and the westward shift of western Pacific subtropical high. Besides, large masses of warm air from low latitude and cold air from high latitude can cause heavy rainfall in Sichuan Basin (Chen et al. 2007).

It is noted that TPV not only influences on the downstream area, but also may interact with other synoptic systems at the leeward slope of the Plateau, inducing heavy rainfall or other weather disasters. Although SWCV is the most representative synoptic system at the leeward slope of the Plateau, its generation, development, and interaction with TPV have not been well understood. Liu and Du (1987) pointed out that when TPV and SWCV are uncoupled, it would inhibit the development of synoptic

system which comes from the leeward slope of the Plateau. But when TPV and SWCV have coupled, it would motivate the synoptic system from the leeward slope of the Plateau. Moreover, when TPV appears above SWCV, SWCV would develop and strengthen, which a view about the coupling of SWCV and TPV is put forward for the first time. About the coupling of TPV and shallow vortex in Sichuan Basin, Chen et al. (2004) indicated that the forcing of TPV's foreside and vertical differential vorticity advection in shallow vortex is a dynamic mechanism, which could stimulate the development of shallow vortex system in Sichuan Basin. Miao (1999) obtained that the interaction of TPV which develops and moves eastward with SWCV is an important way to evoke SWCV development and its heavy rainfall. Zhao and Wang (2010) studied a case that TPV evokes SWCV. It showed that TPV originates and slips down along the northeast side of the Plateau, and induces SWCV occurrence. Under the dynamic condition of forced lifting, the low-level easterly flow caused by eastward moving TPV releases convective available potential energy (CAPE) to produce meso-scale convective system (MCS) with rainfall. Besides, the feedback of condensation heat from precipitation drives the rapid development of SWCV. Meanwhile, TPV growth is mainly affected by surface heat flux and the development of TPV largely determines the formation of SWCV.

However, due to steep terrain of Qinghai-Tibet Plateau, complex underlying surface, and much sparse observation, the previous researches on the interaction of TPV and SWCV and their effects on precipitation are almost case analysis. The mechanism of the two vortices' interaction and their influences is still not clear. So, high-resolution data should be used to carry out systematic and comprehensive research on the typical structure and synoptic process of the two vortices, as well as their influences. In this paper, a rainstorm caused by the merging of TPV and SWCV in Sichuan Basin is comparatively analyzed during 29 June–2 July 2013 by using the conventional observed data, and its time intensive observed data and the intensive observed data during the atmospheric scientific experiment of SWCV in flood season since 2010 (Li et al. 2010, 2011, 2012). Some significant results have been obtained.

## 2 Data and methods

### 2.1 Conventional observed data and its time intensive observed data

The conventional observed data include 397 stations' rainfall data and seven operational sounding stations' meteorological data which are daily obtained at 0000, 1200 UTC during 29 June–2 July 2013. In Sichuan

Province, the seven operational sounding stations are Ganzi (100.00°E, 31.62°N, altitude 3394 m), Hongyuan (102.55°E, 32.80°N, altitude 3493 m), Batang (99.10°E, 30.00°N, altitude 2590 m), Xichang (102.27°E, 27.90°N, altitude 1599 m), Wenjiang (103.87°E, 30.75°N, altitude 549 m), Yibin (104.60°E, 28.80°N, altitude 341 m), and Dazhou (107.50°E, 31.20°N, altitude 344 m).

China Meteorological Administration (CMA) organized the intensive observed period (IOP) at 0600 UTC daily during 1–30 June 2013. It included the fifteen operational observatories in Sichuan, Yunnan, Guizhou, and Chongqing in Southwest China. Among these observatories, seven operational sounding stations are in Sichuan (Ganzi, Hongyuan, Batang, Xichang, Wenjiang, Yibin, and Dazhou), five operational sounding stations in Yunnan (Lijiang, Kunming, Simao, Mengzi, and Tengchong), two operational sounding stations in Guizhou (Weining and Guiyang), and one operational sounding station in Chongqing (Shapingba).

## 2.2 Intensive observed data of SWCV scientific experiment

Based on the previous SWCV scientific experiment (Li et al. 2010, 2011, 2012), Institute of Plateau Meteorology (IPM), CMA, Chengdu, continued the intensive observation scientific experiment of SWCV during 21 June–31 July 2013 (41 days in total). In this SWCV scientific experiment, four sounding stations were added in spatial distribution located in the key areas of SWCV activities, including Jiulong (101.50°E, 29.01°N, altitude 2925 m) in the south of western Sichuan plateau, Mingshan (103.12°E, 30.08°N, altitude 691 m) at the western edge of Sichuan Basin, Jiange (105.31°E, 32.17°N, altitude 544 m) at the northern edge of Sichuan Basin, and Jinchuan (102.07°E, 31.48°N, altitude 2169 m) in the middle of western Sichuan plateau (Fig. 1). According to meteorological observed standards, the new sounding observations are made four times (0000, 0600, 1200, 1800 UTC) daily by GPS sounding system. The meteorological variables included isobaric temperature (K), relative humidity (%), u wind (m/s), v wind (m/s), geopotential height (m), air pressure (hPa), dew point temperature (K), specific humidity (g/kg), wind direction (°), wind speed (m/s), distance (m), longitude (°), and latitude (°). Moreover, in the basis of the conventional observation at 0000, 1200 UTC, the seven operational sounding stations (Ganzi, Hongyuan, Batang, Xichang, Wenjiang, Yibin, and Dazhou) increased two times sounding observations at 0600, 1800 UTC.

## 2.3 Methods

By scientific experiment, observed analysis, and dynamic diagnosis, the comprehensive research about this

rainstorm weather and the vortices' activities is done, especially by using the intensive observed data during the IPM's SWCV scientific experiment and the CMA's IOP. The purpose is to reveal the evolutions of SWCV and TPV, and their precipitation anomalies. Furthermore, the frontogenetical function (Wu 1999) and the potential vorticity (PV) (Ertel 1942) are used to analyze the evolutions of the vortices. And O'Brien's (1970) kinematic method is adopted to calculate vertical velocity. In addition, the Cressman interpolation method is applied, and the interpolation radii are 1, 3, 5, 7, and 10, respectively.

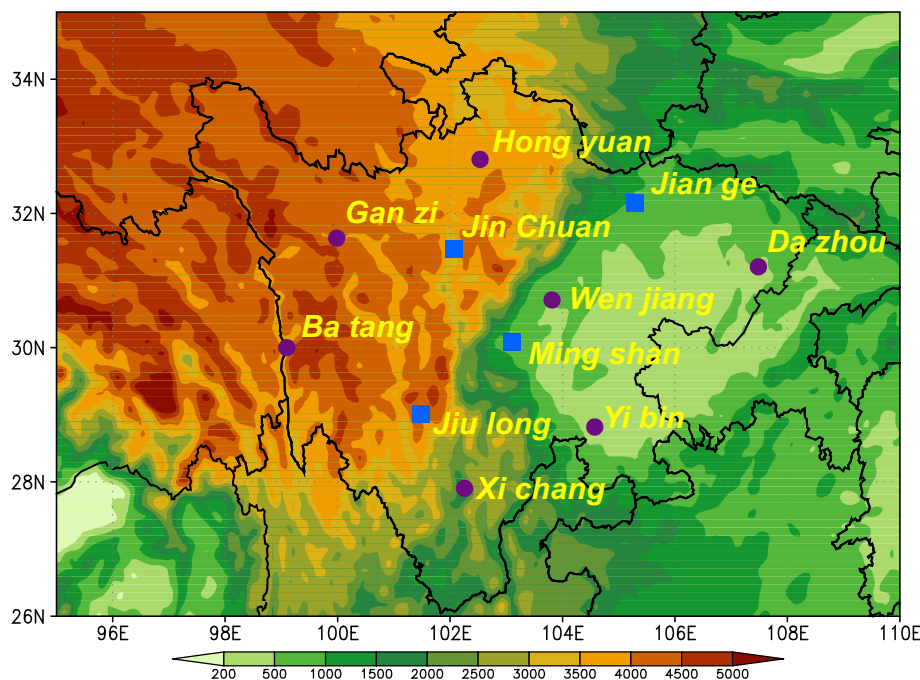
## 3 Atmospheric circulations during precipitation

### 3.1 Rainstorm event

A rainstorm occurred in eastern Sichuan during 29 June–2 July 2013 with 39 stations' precipitation amount >100 mm. The area-averaged precipitation amount of more than 200 mm was observed in Suining, Nanchong, and Deyang. The 72-h accumulated precipitation in Suining reached up to 519.5 mm, which is the historical extreme precipitation in local meteorological record (Fig. 2a).

Before the merging of TPV and SWCV (Fig. 2b), from 0000 UTC to 1200 UTC 29 June, TPV at the border of Qinghai and Sichuan (101.1°E, 32.8°N) moved southeastward to near Heishui (103.5°E, 31.5°N) of western Sichuan plateau without obvious rainfall at 0600 UTC. Then TPV turned north and moved to the north of western Sichuan plateau (102.8°E, 33.3°N) at 1200 UTC. There was light rain in western Sichuan plateau, and the 6-h accumulated precipitation of 10.8 mm was observed in Rangtang (100.1°E, 32.3°N). Meanwhile, SWCV originated in Muli (100.8°E, 28.2°N) on the south of Jiulong and stayed at its source without rainfall. From 0600 UTC to 1200 UTC 29 June, SWCV moved northeastward to southern Ya'an (102.4°E, 29.3°N), small-scale rainfall occurred in Mianning (102.4°E, 29.2°N) where the 6-h accumulated precipitation reached 24.9 mm. From 1200 UTC 29 to 0000 UTC 30 June, SWCV moved along northeastward path to Meishan (104.1°E, 30.2°N). A rainfall was obvious at northeast–southeast quadrant of SWCV and the heavy rainfall of 132 mm in 12 h was recorded at Zigong (104.8°E, 29.4°N) in eastern Sichuan. At the same time, TPV moved along eastward path to southeastern Gansu (105.0°E, 33.2°N). Influenced by TPV and SWCV, heavy rainfall occurred in northwest-central-southeast Sichuan Basin, mainly located at the east of SWCV. The 12-h precipitation in Jintang (104.4°E, 30.9°N), Chengdu, reached 160.9 mm.

**Fig. 1** The distribution of terrain and sounding stations (blue rectangles represent the space–time intensive observed stations of SWCV, purple solid rounds represent the operational conventional observed stations, and shaded areas represent different altitudes, unit: m)



At the merging stage of the two vortices (Fig. 2c), from 0000 UTC to 0600 UTC 30 June, the northeastward moving SWCV and the southward moving TPV merged with each other, strengthened, and formed a combined vortex (CBV, defined by the vortex at 500 hPa) in northwestern Sichuan Basin (104.9°E, 32.0°N) at 0600 UTC, causing heavy rainfall in central-east Sichuan Basin. A rain belt developed around the south and east of CBV to the border of Sichuan and Chongqing, and the 6-h accumulated precipitation in Suining (105.55°E, 30.50°N) reached 185.2 mm. This was the strongest precipitation during the rainstorm weather.

During CBV southward motion (Fig. 2d), from 0600 UTC to 1200 UTC 30 June, CBV moved along southward path to near Chengdu (104.5°E, 30.9°N), rainfall remained at the east side of it, and the 6-h accumulated precipitation in Suining reached 121.9 mm again. And during CBV southeastward motion (Fig. 2e), from 1200 UTC 30 June to 0000 UTC 1 July, CBV arrived the eastern Sichuan (105.7°E, 30.5°N). With the CBV movement, the 195.5 mm heavy rainfall in 12 h occurred in Tongliang (106.07°E, 29.85°N), Chongqing at the south of CBV. From 0000 UTC to 1200 UTC 1 July, CBV stayed at eastern Sichuan, the precipitation at the border of Sichuan and Chongqing reduced, but heavy rainfall of 81.2 mm occurred in Suining at the west side of CBV. During CBV movement northward (Fig. 2f), from 1200 UTC 1 to 0000 UTC 2 July, CBV moved northwestward and then turned to the northeast at 1800 UTC 1 July, and arrived at the border of Sichuan and Shanxi and weakened. Because

CBV and its rainfall advance out of Sichuan, the rainstorm in eastern Sichuan basically ended.

### 3.2 Atmospheric circulation pattern

The atmospheric circulation pattern of this rainstorm shows (figures omitted) before the two vortices' merging, at 0000 UTC 29 June, at 500 hPa, there was a large transverse trough in the mid-high latitude region of Eurasia. The westerly flow occupied northern China, a series of quick-moving short-wave troughs from the north of Tibetan Plateau moved to its downstream area and TPV moved to the border of Qinghai and Sichuan with 500 hPa westerly troughs. At 700 hPa, a shallow trough existed in southwest China, and SWCV originated in Muli on the south of Jiu-long. At 1200 UTC 29 June, TPV moved slowly with 500 hPa low trough to the north of western Sichuan plateau where a closed low center appears. At the same time, at 700 hPa, the shallow trough in southwest China developed and strengthened, and SWCV moved slowly along the northeastward path to southern Ya'an. At 0000 UTC 30 June, at 500 hPa, the transverse trough in the mid-high latitude region of Eurasia continued to intensify, and TPV moved eastward to southeastern Gansu with low trough. And at 700 hPa, the shallow trough developed eastward and SWCV moved to western Sichuan Basin. At the stage of the two vortices' coupling at 0600 UTC 30 June, SWCV and TPV merged into one vortex CBV, and strengthened in northwestern Sichuan Basin. And there appeared strong low center at both 700 and 500 hPa. After the two vortices'



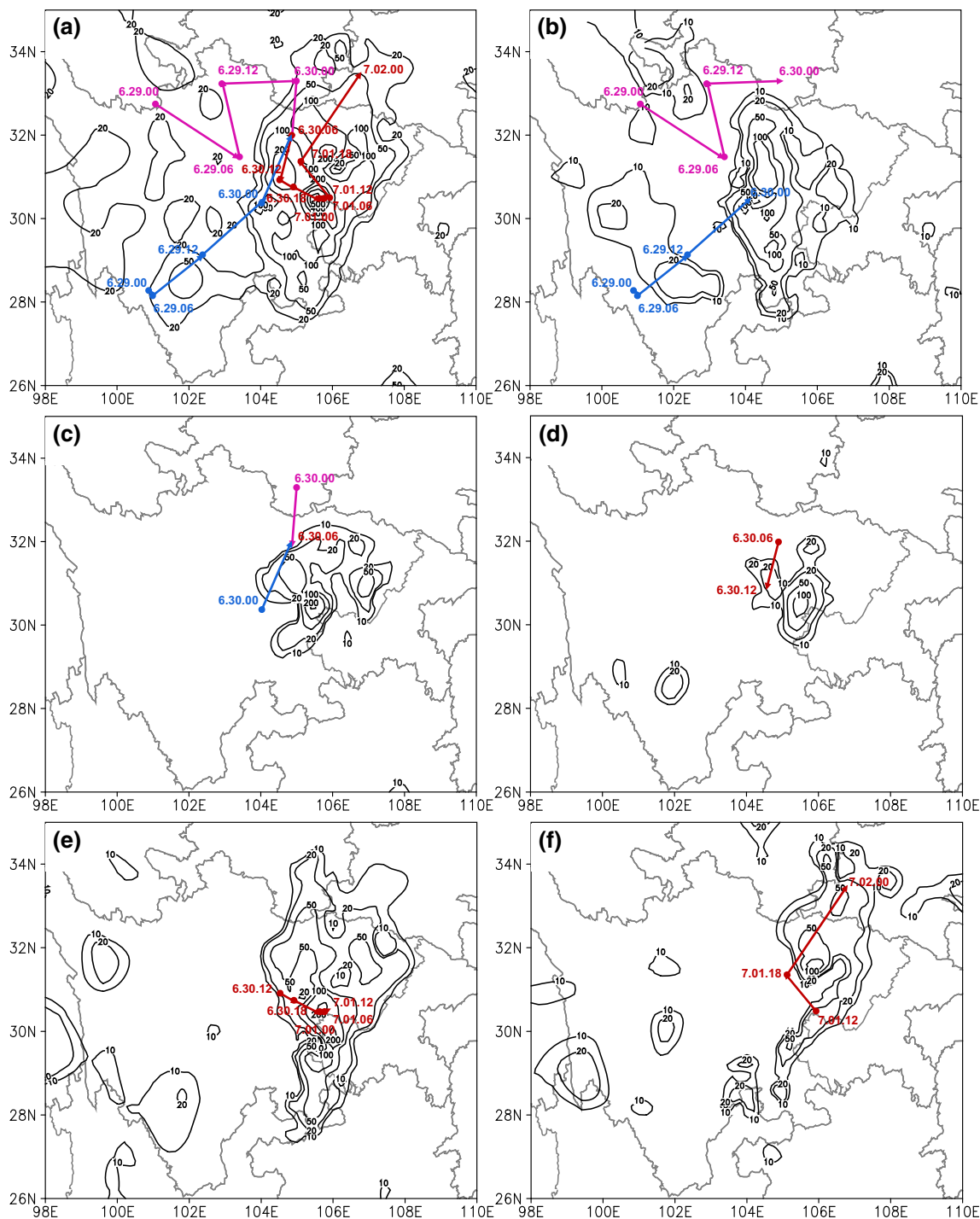


**Fig. 2** The precipitation (contour, unit: mm) and motion path of vortices (pink arrows represent TPV motion path at 500 hPa, blue arrows represent SWCV motion path at 700 hPa and orange arrows represent CBV motion path at 500 hPa): **a** 0000 UTC 29 June to 0000

UTC 2 July 2013; **b** 0000 UTC 29 to 0000 UTC 30 June; **c** 0000 UTC to 0600 UTC 30 June; **d** 0600 UTC to 1200 UTC 30 June; **e** 1200 UTC 30 June to 1200 UTC 1 July; **f** 1200 UTC 1 to 0000 UTC 2 July

merging, the trough at 500 hPa maintained over Sichuan Basin, and CBV moved southward slowly. Meanwhile, the closed low center at 700 hPa disappeared gradually, and a trough originated in Sichuan Basin again. From 1200 UTC 30 June to 0000 UTC 1 July, because the western Pacific

subtropical high retreated eastward, CBV moved south-eastward, and the trough at 700 hPa continually advanced to the border of Sichuan, Guizhou, and Chongqing. But, from 0000 UTC to 1200 UTC 1 July, CBV stayed at eastern Sichuan with little movement due to the advance

northward of the western Pacific subtropical high again. Afterward, because of the stabilization of the western Pacific subtropical high, CBV weakened and moved northward, and the trough at 500 hPa moved northeastward to Dazhou in Sichuan, and the trough at 700 hPa remained at the border of Sichuan and Chongqing. During the CBV extinction, at 0000 UTC 2 July, the transverse trough at 500 hPa in the mid-high latitude region of Eurasia weakened and there appeared the large-scale circulation pattern of “two troughs and one ridge.” The flat westerly flow in northern China did not exist and CBV gradually weakened.

### 3.3 Water vapor transport and convergence

Rainfall needs a favorable circulation condition and plenty of water vapor. Fig. 3b1 shows the averaged water vapor distribution during rainstorm with the conventional plus intensive observed data. At 700 hPa, the vapor mainly came from low-latitude South China Sea and the Bay of Bengal. The large water vapor transport flux distributed along the northeast–southeast edge of Sichuan. There

existed a large water vapor flux divergence area in Jiulong, and a water vapor flux convergence center of  $-5 \times 10^{-8} \text{ g hPa}^{-1} \text{ cm}^{-2} \text{ s}^{-1}$  was in southern Sichuan Basin and it had a good correspondence with rainfall area. But, only with the conventional observed data (Fig. 3a1), it shows that strong water vapor transport flux areas not only existed along the northeast–southeast edge of Sichuan but also in central-west Sichuan. Meanwhile, an unreal strong water vapor flux convergence of  $-9 \times 10^{-8} \text{ g hPa}^{-1} \text{ cm}^{-2} \text{ s}^{-1}$  appeared in western Sichuan, and no significant rainfall occurred correspondingly in this area.

At 850 hPa, with the conventional plus intensive observed data (Fig. 3b2), it shows that because of the obstruction of Hengduan Mountain and Yunnan–Guizhou Plateau, water vapor transport was mainly from the South China Sea and the large water vapor flux was in northeastern Sichuan and Chongqing. A belt of strong water vapor flux convergence existed in northeastern Sichuan and the Yunnan–Guizhou border where two large convergence centers are all  $-7 \times 10^{-8} \text{ g hPa}^{-1} \text{ cm}^{-2} \text{ s}^{-1}$ . The one in northeastern Sichuan was at the border of Suining and

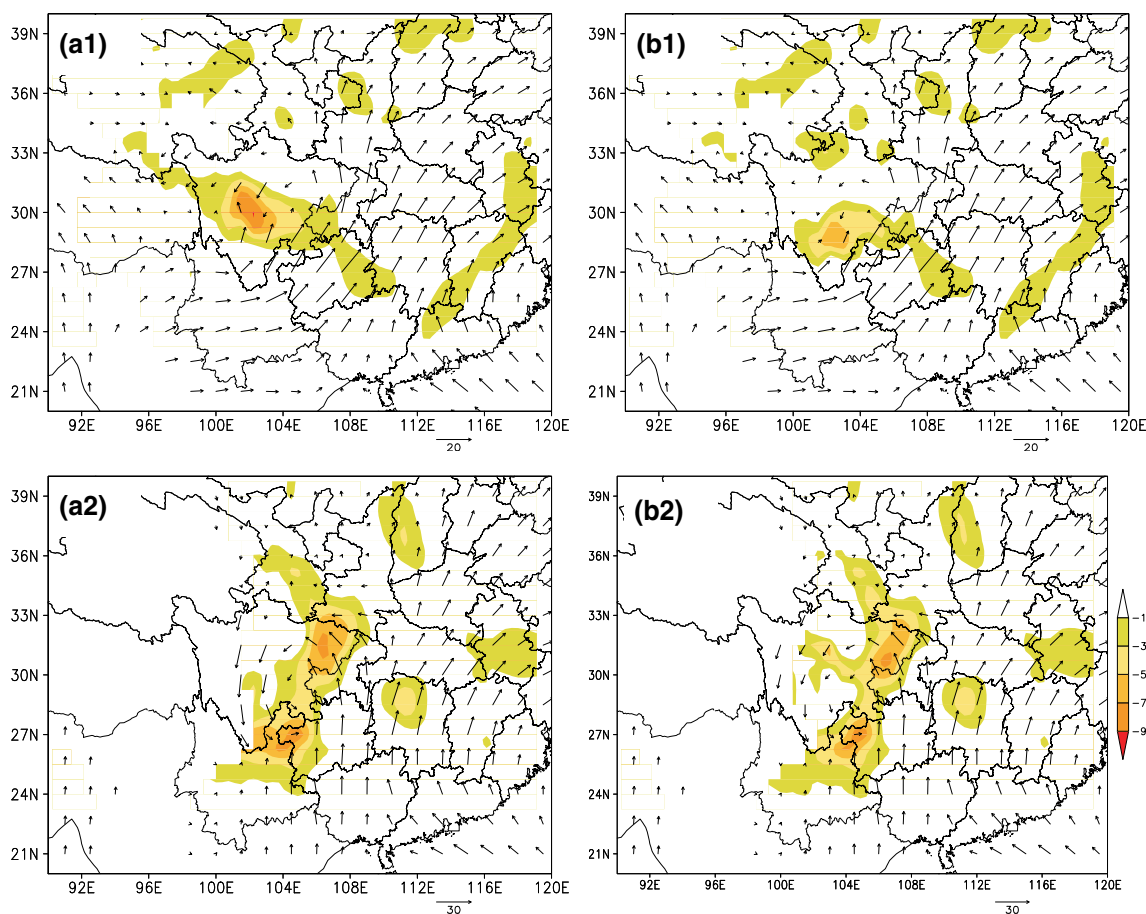


**Fig. 3** The averaged water vapor transport (vector, unit:  $10^{-3} \text{ g cm}^{-1} \text{ hPa}^{-1} \text{ s}^{-1}$ ) and water vapor flux divergence (shaded, unit:  $10^{-8} \text{ g hPa}^{-1} \text{ cm}^{-2} \text{ s}^{-1}$ ) during rainstorm process (**a1**, **a2** based on

the conventional observed data; **b1**, **b2** based on the conventional plus intensive observed data): **a1** 700 hPa; **b1** 700 hPa; **a2** 850 hPa; **b2** 850 hPa

Nanchong where heavy rainfall occurs. Only with the conventional observed data (Fig. 3a2), compared with the conventional plus intensive observed data, it indicates that the above strong water vapor flux convergence belt was exaggerated, especially the two large convergence centers, and the large water vapor flux convergence areas did not well correspond with the actual heavy rainfall.

## 4 Evolutions of the two vortices

During the rainstorm, the effects of SWCV and TPV were very important. Therefore, the evolutions and developments of the two vortices were analyzed as follows.

### 4.1 Vortices' evolutions before merging

Figure 4 shows the weather map at 700 hPa from 0000 UTC 29 to 0000 UTC 30 June. It shows that at 0000 UTC 29 June (Fig. 4b1) with the conventional plus intensive observed data, before the two vortices' merging, a shallow trough appeared in southern Sichuan. The north-central Sichuan Basin was controlled by a wide range of cold air, some cold air had invaded into southern Sichuan, the temperature at Jiulong dropped to 13 °C, and the wind field in Xichang, Jiulong, and Lijiang formed a cyclonic center in Muli (100.8°E, 28.2°N) on the south of Jiulong, which means SWCV occurrence. However, only with the conventional observed data (Fig. 4a1), it shows cold air existed only in north-central Sichuan. And without the intensive observed data at Jiulong, the wind field could not reveal the cyclonic center (newborn SWCV) in Muli on the south of Jiulong. At 0600 UTC 29 June (Fig. 4b2) with intensive observed data, the shallow trough in southern Sichuan maintained and weakened. The geopotential height in Jiulong decreased rapidly from 3070 to 3050 gpm. Under the control of warm air in western Sichuan plateau, the temperature in Jinchuan and Jiulong increased to 15 and 20 °C, respectively, and there was a warm center in the southern Chongqing. Furthermore, the cyclonic center in Muli still remained with a southerly flow in Sichuan. But there is no conventional observation at 0600 UTC. At 1200 UTC 29 (Fig. 4b3) with the conventional plus intensive observed data, western Sichuan plateau was influenced continuously by a low system, which causes the geopotential height in Jinchuan to drop to 3040 gpm and the shallow trough to disappear, being replaced by weak ridge at the southern Sichuan. With warm air movement northward, the most of Sichuan became strong warm areas except for northwestern Sichuan Basin. Especially, the southerly in Jiulong turned into the northerly, SWCV moved from Muli to near Ya'an. Due to the lack of the intensive observed data, the conventional observed data (Fig. 4a3) show that

strong cold air stayed in northern Sichuan, but could not reflect the existence of SWCV and its variations. At 1800 UTC 29 (Fig. 4b4) with the intensive observed data, the geopotential height formed a saddle-pattern field in Sichuan with warmer air of the most it. But, because of cold air invading into northeastern Sichuan, the temperature in Dazhou rapidly decreased from 15 to 12 °C. The wind direction in Jiulong turned into easterly, which induces SWCV to weaken. It must be pointed out that there is no conventional observation at 1800 UTC. At 0000 UTC 30 (Fig. 4b5) with the conventional plus intensive observed data, the strongly developed TPV extended from 500 hPa down to 700 hPa, and there appeared a closed low center at the border of Sichuan and Gansu. At the same time, SWCV moved northeastward into Sichuan Basin with 3050 gpm closed low center. In temperature field, TPV was present as a cold center at 700 hPa, which is less than 8 °C. Cold air continued to invade into northeastern and southern Sichuan Basin, and the temperature in Jiulong dropped to 11 °C and became a cold center. Affecting by leading flow with TPV movement, the wind direction in Jiulong, Mingshan, and Chengdu all turned from southerly to northerly, which formed a strong wind shear line combining with the southerly flow at the border of Sichuan and Chongqing, and SWCV developed and strengthened. But, without the intensive observation, the conventional observed data (Fig. 4a5) only show a wide range of low center in northwestern Sichuan, and it could not exhibit the existence of both SWCV and the cold center over Jiulong. Moreover, it cannot reflect the wind shear line clearly.

Figure 5 shows the weather map at 500 hPa from 0000 UTC 29 to 0000 UTC 30 June. It shows that at 0000 UTC 29 (Fig. 5b1) with the conventional plus intensive observed data, before the two vortices' merging, it could be seen that a low trough existed in northwestern Sichuan. The geopotential height in Ganzi, Hongyuan, and Jinchuan all dropped to 5010 gpm. With cold air invading into northern Sichuan, the wind field in western Sichuan plateau was westerly flow. The wind in Ganzi, Hongyuan, and Jinchuan formed a cyclonic center. Meanwhile, TPV moved to the margin of Sichuan. Without the intensive observation, the conventional observed data (Fig. 5a1) show that the <5810 gpm cyclonic center was not very clear and the range of cold air invading northern Sichuan was relatively larger. At 0600 UTC 29 (Fig. 5b2) with the conventional plus intensive observed data, TPV moved into western Sichuan plateau and produced a <5820 gpm closed low with a cold center. With TPV development and southeastward movement, northerly appeared at the southwest side of TPV in western Sichuan plateau. But there is no conventional observation at 0600 UTC. At 1200 UTC 29 (Fig. 5b3) with the conventional plus intensive observation, TPV moved northward to near Nuorgai (102.8°E, 33.3°N),

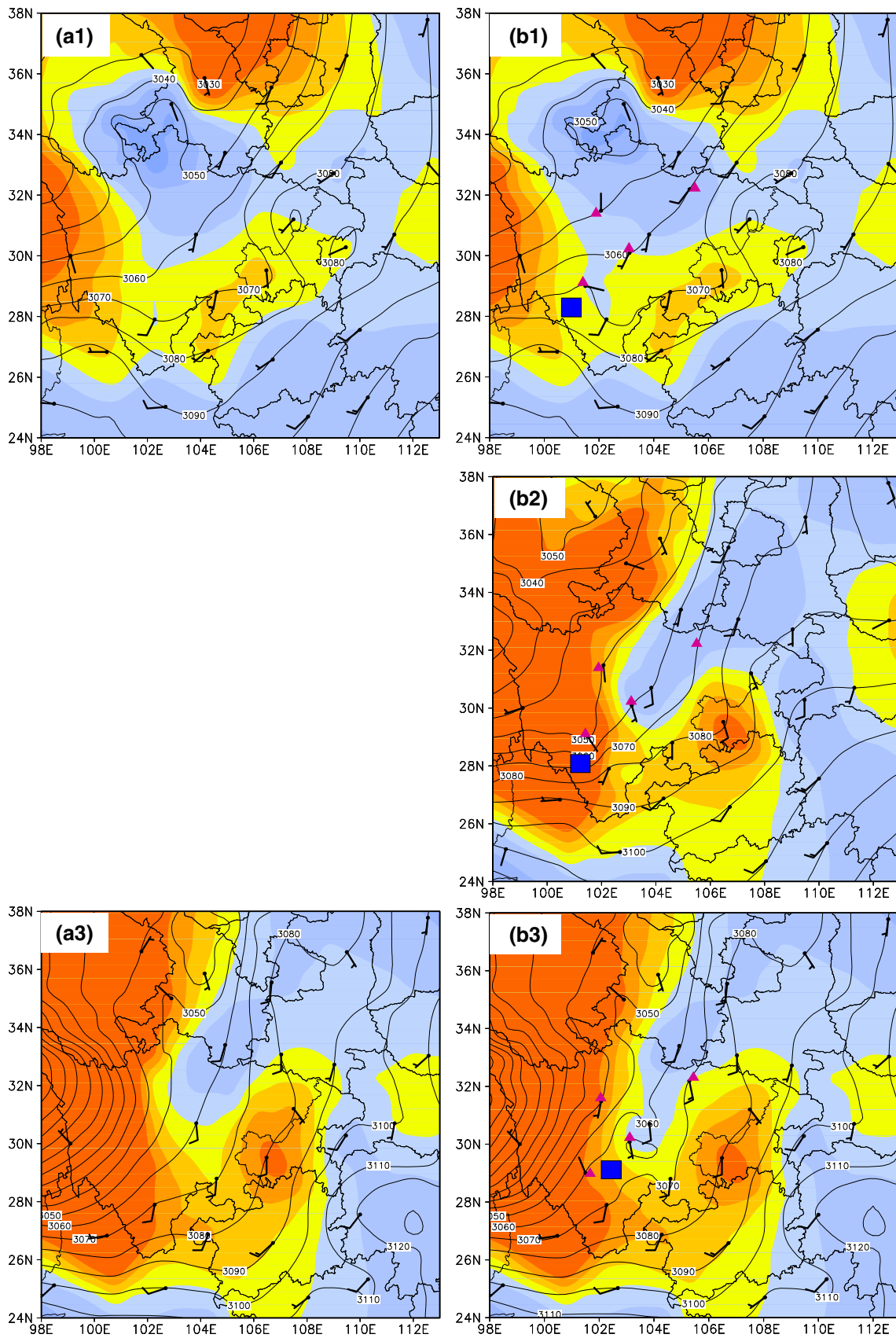




**Fig. 4** The geopotential height (contour, unit: gpm), temperature (shaded, unit: °C), and wind (vector, unit: m/s) at 700 hPa from 0000 UTC 29 to 0000 UTC 30 June 2013 (purple triangles represent the space-time intensive observed stations of SWCV, blue rectangle represents the SWCV center; **a1–a5** based on the conventional observed data; **b1–b5** based on the conventional plus intensive observed data). **a1** 0000 UTC 29; **a3** 1200 UTC 29 June; **a5** 0000 UTC 30 June; **b1** 0000 UTC 29; **b2** 0600 UTC 29; **b3** 1200 UTC 29; **b4** 1800 UTC 29 June; **b5** 0000 UTC 30 June

the geopotential height in Hongyuan dipped to 5810 gpm. And there was a shallow trough in the southeastern Sichuan Basin. When warm air extends eastward into the west and south of TPV, its cold center became small and there was mainly westerly flow over western Sichuan plateau. However, the conventional observation (Fig. 5a3) shows that the position of TPV was relatively south and no cold air advanced into the east of it. At 1800 UTC 29 (Fig. 5b4) with the intensive observation, the trough in southeastern Sichuan developed and deepened with the cold area. But

there is no conventional observation at 1800 UTC. At 0000 UTC 30 (Fig. 5b5) with the conventional plus intensive observed data, TPV moved to southeastern Gansu with the center dropped to 5760 gpm, and the trough on the south of it intensified and the geopotential height in Mingshan decreased from 5840 to 5820 gpm. The cold center of TPV dropped to <math>-3\text{ }^\circ\text{C}</math>, and the developing TPV brought strong northerly to west-central Sichuan. But with the conventional observed data (Fig. 5a5), it shows that TPV low center extended more largely, and the influence range of cold center was relatively larger.

### 4.2 Vortex’s evolutions after merging

#### 4.2.1 CBV movement southward

Figure 6 shows the weather map at 700 hPa from 0600 UTC 30 to 1200 UTC 30 June. At 0600 UTC 30

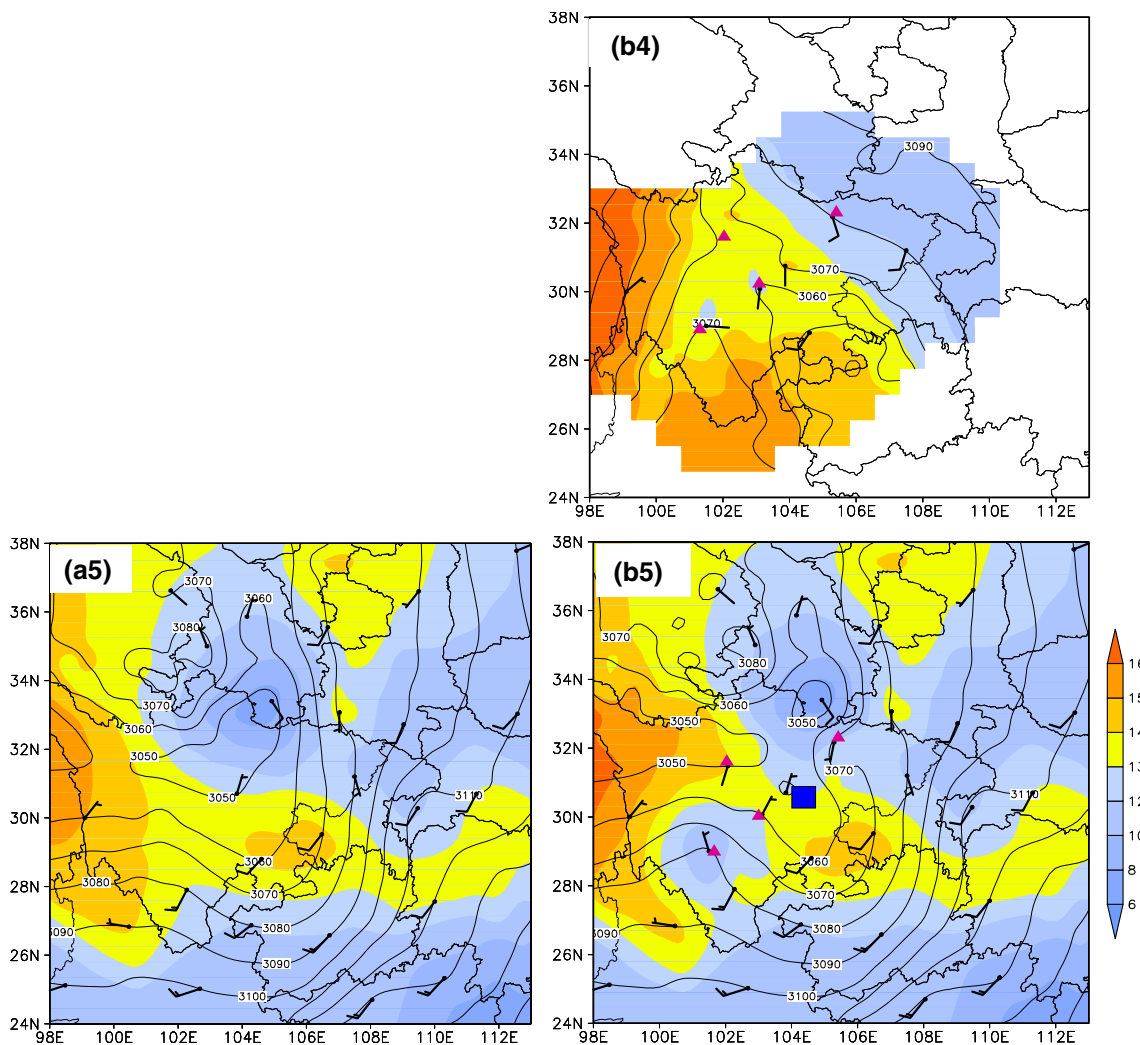


**Fig. 4** continued

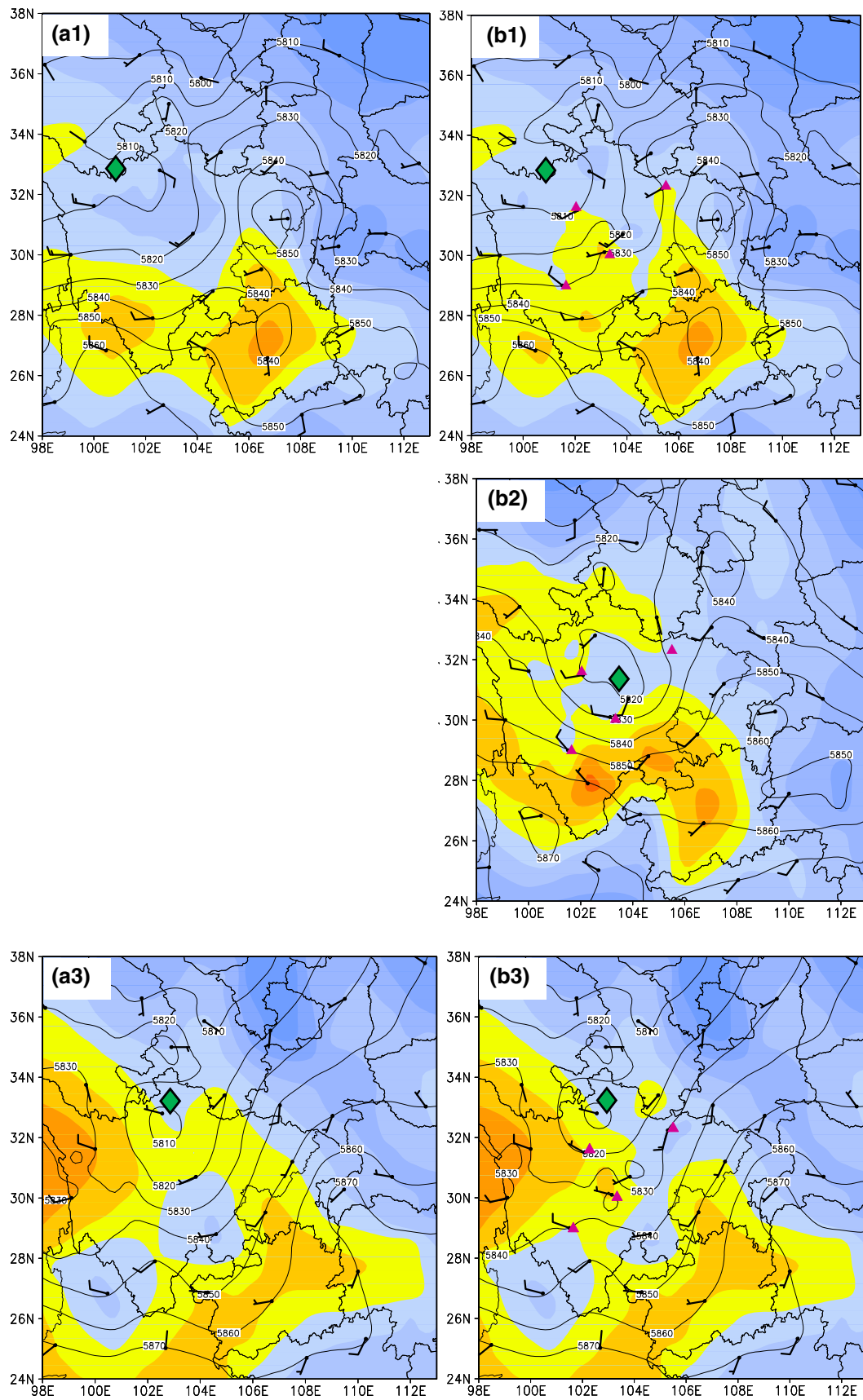


**Fig. 5** The same as Fig. 4, but for 500 hPa. The *green rhombus* represents the TPV center

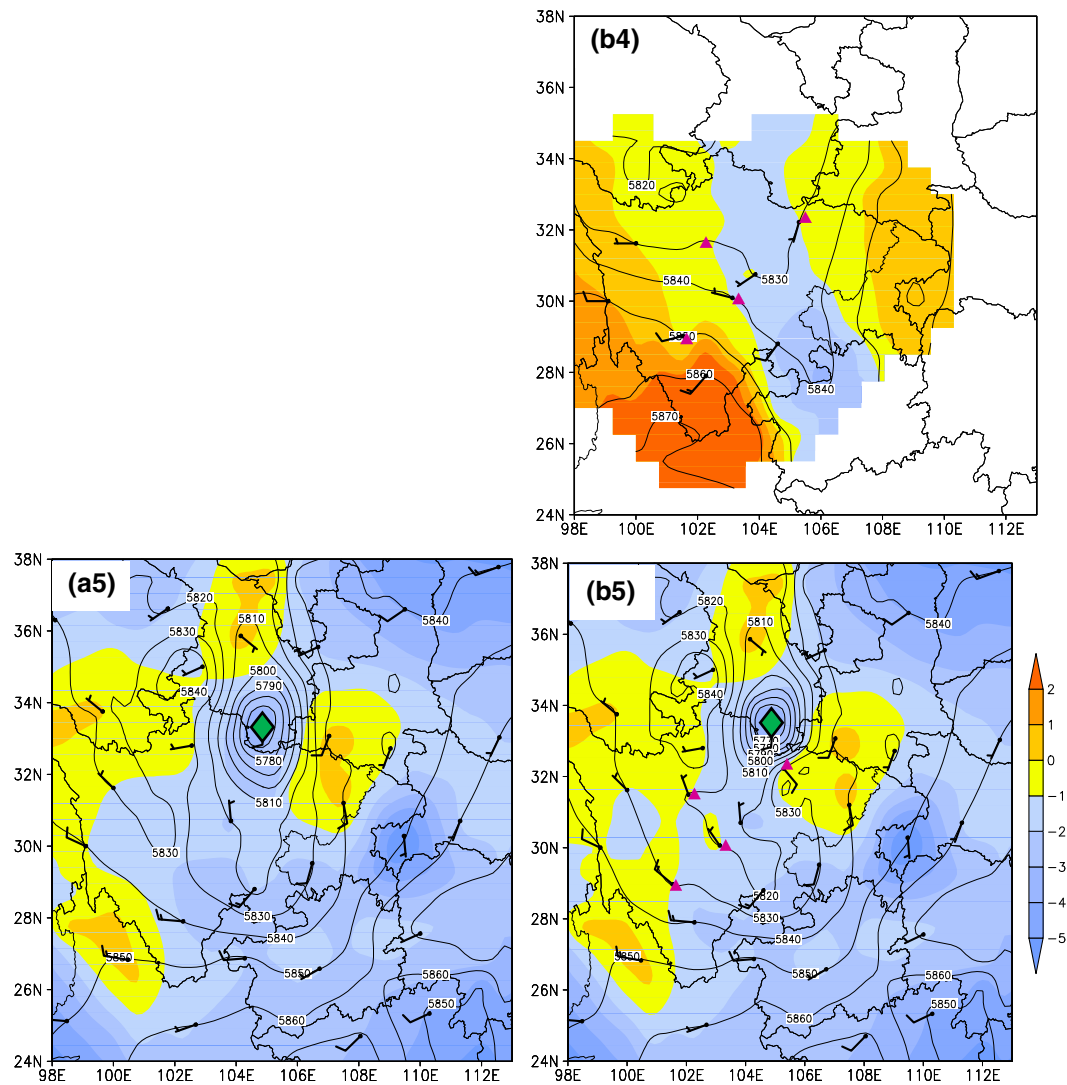


**Fig. 5** continued

(Fig. 6b1) with the intensive observed data, during the two vortices' merging, it could be seen that along with the movements of both SWCV northeastward and TPV southward, the two vortices met in the northwestern Sichuan Basin and merged each other and strengthen strongly, which forms a much deep vortex CBV. At the moment, CBV center dropped to 3000 gpm and 6 °C. The cyclonic circulation enhanced around CBV accompanied by heavy rainfall. But, at 0600 UTC there is no the conventional observation, which cannot reflect the process of the two vortices' merging into one vortex. At 1200 UTC 30 (Fig. 6b2) with the conventional plus intensive observed data, during CBV movement southward, it weakened in west-central Sichuan Basin, the closed contours disappeared with a weak cyclonic circulation, the cold-core structure was destroyed, and the geopotential height in Jiange increased from 3010 to 3070 gpm. But the

conventional observed data (Fig. 6a2) show that the low system in western Sichuan plateau was relatively weaker, and the range of cold air in western Sichuan Basin was larger and the weak cyclonic circulation did not exist to become a wind shear.

Figure 7 shows the weather map at 500 hPa from 0600 UTC 30 to 1200 UTC 30 June. At 0600 UTC 30 (Fig. 7b1) with the intensive observed data, during the two vortices' merging, it could be seen that it is the same as at 700 hPa, TPV moved southward and SWCV moved northeastward, and merged each other in northern Sichuan Basin, which forms a strong deep vortex system CBV. The low center reached 5700 gpm and a cold-core structure appeared again with  $<-4$  °C. And there existed a clear cyclonic circulation around CBV. But there is no conventional observation at the moment. At 1200 UTC 30 (Fig. 7b2) with the conventional plus intensive observed data, during CBV

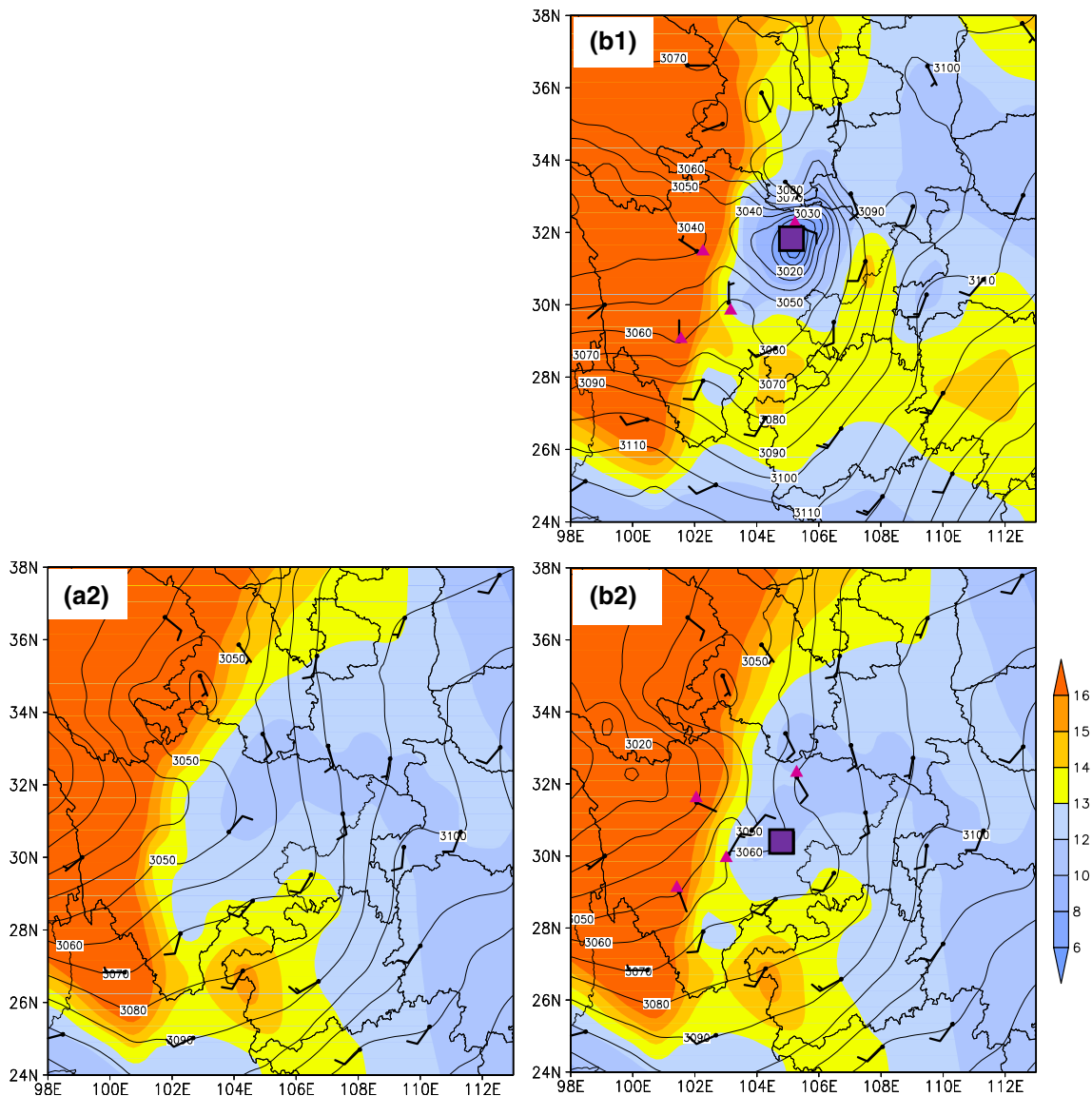


**Fig. 6** The geopotential height (contour, unit: gpm), temperature (shaded, unit: °C), and wind (vector, unit: m/s) at 700 hPa from 0600 UTC 30 to 1200 UTC 30 June (purple triangles represent the space-time intensive observed stations of SWCV, purple rectangle

represents the CBV center at 700 hPa; **a2** based on the conventional observed data; **b1–b2** based on the conventional plus intensive observed data). **b1** 0600 UTC 30; **a2** 1200 UTC 30; **b2** 1200 UTC 30 June

movement southward, it was to near Chengdu and weakened obviously. Its geopotential height rose to 5810 gpm, and the intensity of cold center decreased, but its closed center still existed. Furthermore, the warm air over western Sichuan plateau extended to Sichuan Basin and came into the center of CBV. Only with the conventional observed data (Fig. 7a2), the intensity of CBV was relatively weaker, and the center of it was more toward north.

#### 4.2.2 CBV movement eastward

At 700 hPa (Fig. 8b1), at 1800 UTC 30 June with the intensive observed data, during CBV movement eastward,

it could be seen that the cyclonic center of CBV existed near Suining and had a cold center. And it is the cold area in northeastern Sichuan. But there is no conventional observation at 1800 UTC. At 0000 UTC 1 July with the conventional plus intensive observed data (Fig. 8b2), CBV moved to eastern Sichuan and strengthened. A closed contour appeared in east-central Sichuan, and the geopotential height in Mingshan decreased from 3060 to 3040 gpm. With the cold air invading into southeastern Sichuan and Chongqing, a cyclonic wind shear appeared at the border of Sichuan and Chongqing. But the conventional observed data (Fig. 8a2) show that the position of CBV center was relatively unclear and the intensity of warm air



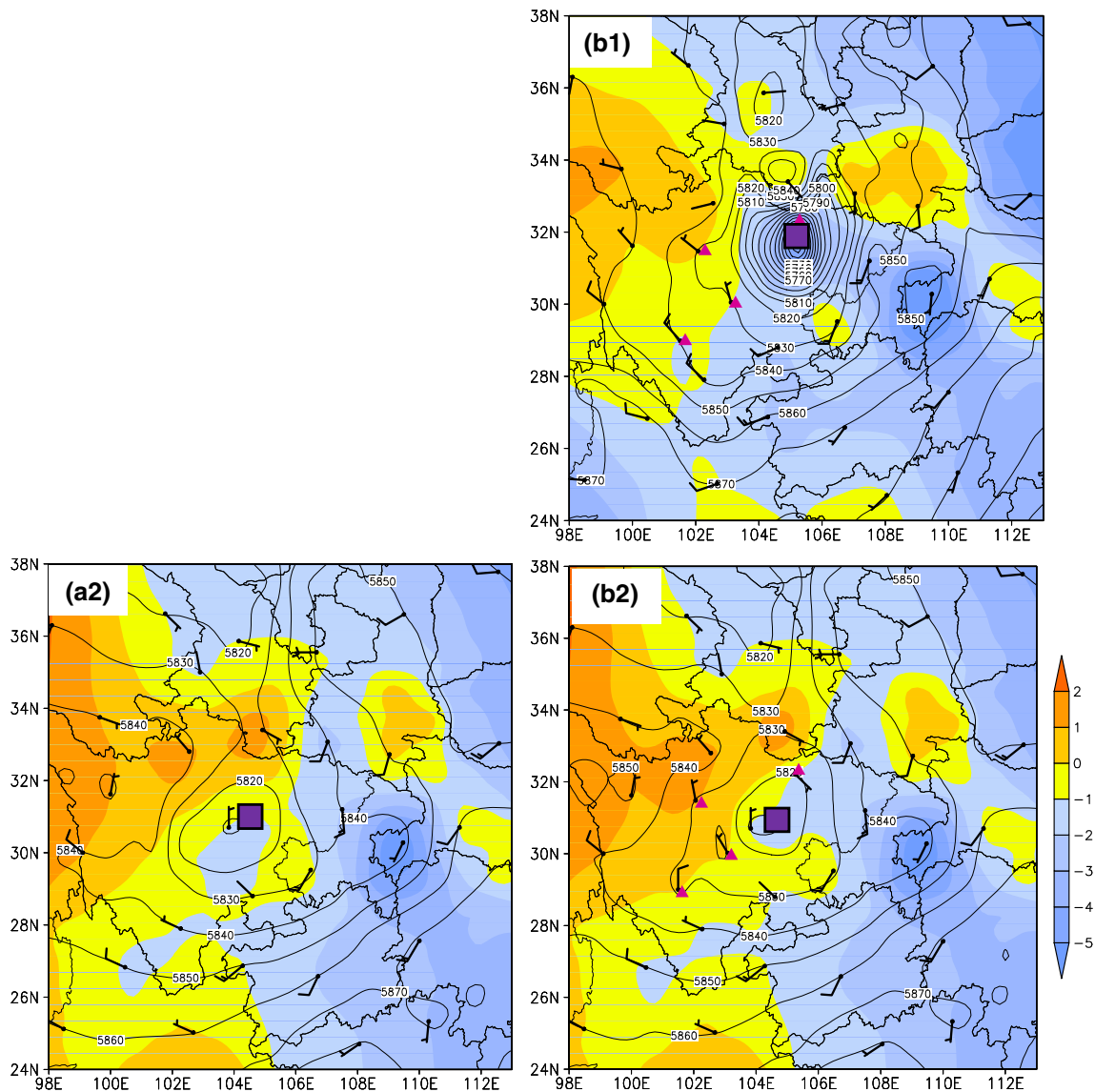


**Fig. 7** The same as Fig. 6, but for 500 hPa. The purple rectangle represents the CBV center at 500 hPa

in western Sichuan plateau was weaker. At 0600 UTC 1 July with the intensive observed data (Fig. 8b3), CBV stayed in eastern Sichuan and weakened, but the low system in western Sichuan plateau developed and strengthened. The geopotential height in Jinchuan dropped to 3030 gpm, and the warm air enhanced in western Sichuan. But there is no conventional observation at 0600 UTC. At 1200 UTC 1 July with the conventional plus intensive observed data (Fig. 8b4), CBV moved little and developed, and a strong low center appeared in western Sichuan plateau. Meanwhile, the geopotential height in Jinchuan rapidly dipped to 3000 gpm. There still existed a cyclonic circulation in northeastern Sichuan Basin. However, the conventional observed data (Fig. 8a4) show there was not low center in western Sichuan plateau and the range of warm air in west-central Sichuan was obviously smaller. At

500 hPa (Fig. 9b1), at 1800 UTC 30 June with the intensive observed data, during CBV movement eastward, it shows that CBV moved to near Santai (105.1°E, 31.1°N) with the low geopotential height in Sichuan Basin and the invasion of cold air weakened in northeastern Sichuan. But there is no conventional observation at the moment. At 0000 UTC 1 July with the conventional plus intensive observed data (Fig. 9b2), CBV moved eastward slowly, it reached 5800 gpm, and two closed low centers existed inside and the one in Chongqing was the main center. But the conventional observed data (Fig. 9a2) show there existed only one closed low center inside, and did not reveal the warm area in northwestern Sichuan Basin. At 0600 UTC 1 July with the intensive observed data (Fig. 9b3), CBV weakened and its closed contour disappeared. The warm air invaded southeastward into the CBV

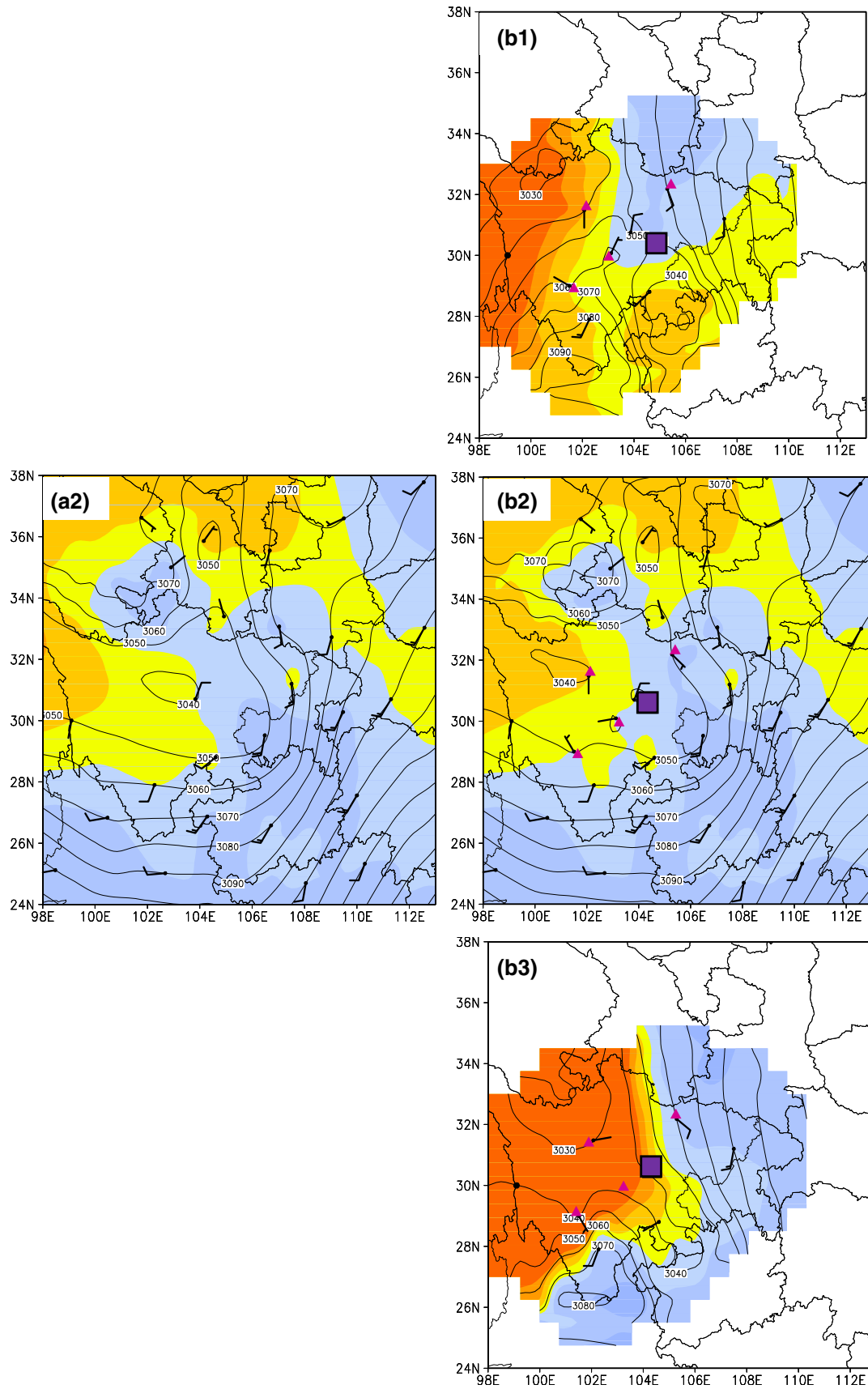


**Fig. 8** The geopotential height (contour, unit: gpm), temperature (shaded, unit: °C), and wind (vector, unit: m/s) at 700 hPa from 1800 UTC 30 to 1200 UTC 1 July (purple triangles represent the space-time intensive observed stations of SWCV, purple rectangle represents the CBV center at 700 hPa; **a2–a4** based on the conventional observed data; **b1–b4** based on the conventional plus intensive observed data). **a2** 0000 UTC 1 July; **a4** 1200 UTC 1 July; **b1** 1800 UTC 30 June; **b2** 0000 UTC 1 July; **b3** 0600 UTC 1 July; **b4** 1200 UTC 1 July

center and made its cold center vanishing. But there is no conventional observation at 0600 UTC. At 1200 UTC 1 July with the conventional plus intensive observed data (Fig. 9b4), CBV stayed in eastern Sichuan and enhanced with the closed contour again. The geopotential height in Dazhou dropped to 5810 gpm, and the warm center became weak. However, the conventional observed data (Fig. 9a4) show that the range of CBV was evidently larger and did not reflect the small-scale cold and warm areas. At 1800 UTC 1 July with the intensive observed data (Fig. 9b5), CBV moved northward and weakened, but without the conventional observation at the moment. Afterward, from 1800 UTC 1 to 0000 UTC 2 July (Fig. 9b6), CBV arrived northward at southwestern Shanxi, its geopotential height increased, and the cyclonic circulation in CBV gradually disappeared. But the conventional observed data (Fig. 9a6) show that the warmer flow was weaker in northern Sichuan Basin.

## 5 Vertical structures of the two vortices

### 5.1 Vertical structures before merging

Because the developing vortex varies quickly on the vertical direction, it is particularly important to study the

vertical structure of vortex. At 0000 UTC 30 June, before the two vortices' merging, at the divergence field with the conventional plus intensive observed data (Fig. 10d), it could be seen that SWCV near 30°N at 700 hPa exhibited strong and deep convergence in the middle and lower troposphere (1000–450 hPa) with the center at 600 hPa and divergence in upper troposphere (400–100 hPa) with the center at 200 hPa. Under the configuration of low-level convergence and up-level divergence, ascending motion expanded widely from surface to 150 hPa and heavy rainfall areas were near 29°N–32°N. And below 700 hPa, the upward flow came from the side slope of southern Sichuan Basin, and above 700 hPa, it came from the southerly over Yunnan–Guizhou Plateau which turns to upward flow at the side slope of southern Sichuan Basin. The ascending motion in SWCV turned into northerly flowing to the low latitude at 150 hPa. Moreover, there was deep southward-slantwise convergence column from surface to 150 hPa with the near-surface convergence center in southern Gansu and the upper convergence center at 250 hPa at the border of Gansu and Sichuan. TPV near 34°N at 500 hPa was located at convergence area just over the near-surface convergence center and there was a weak divergence area around 300 hPa over TPV, and a divergence center was at 700 hPa over the side slope of northern Sichuan Basin. The ascending motion around TPV exhibited a kind of slantwise upward flow from the south to north along the side slope topography of northern Sichuan Basin and the southern Gansu. The above shows that SWCV in Sichuan Basin was a deep system and stronger than TPV in Gansu. However, only with the conventional observed data (Fig. 10a), the most difference from Fig. 10d is that the upper convergence center at 250 hPa on the south of TPV did not exist and became a divergence area

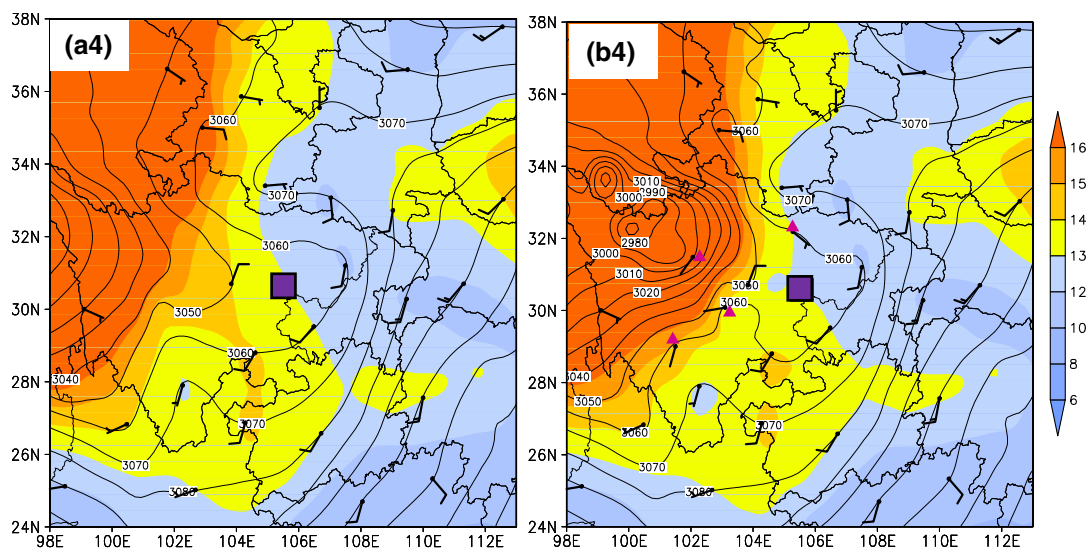


**Fig. 8** continued

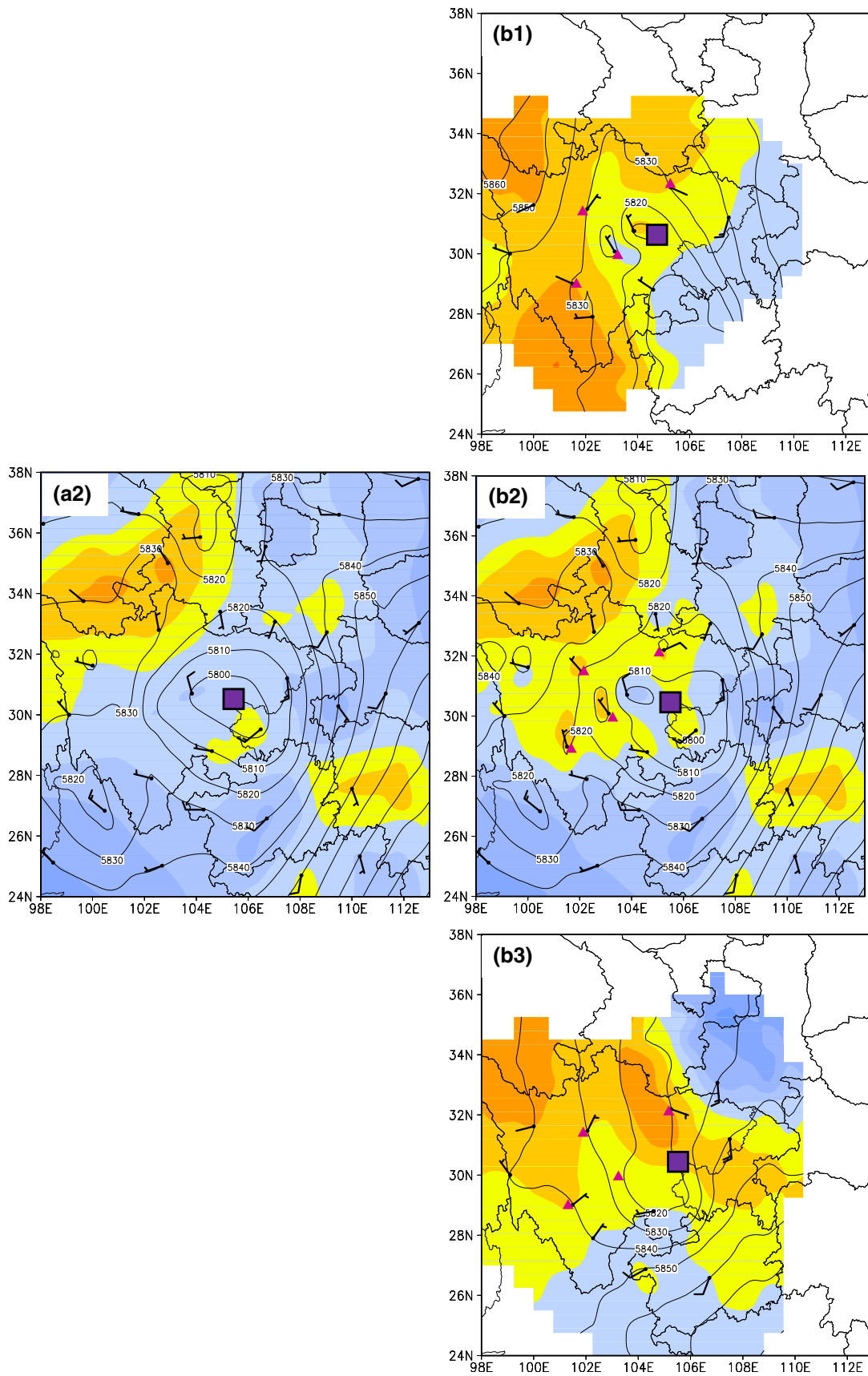




**Fig. 9** The geopotential height (contour, unit: gpm), temperature (shaded, unit: °C), and wind (vector, unit: m/s) at 500 hPa from 1800 UTC 30 to 0000 UTC 2 July (purple triangles represent the space-time intensive observed stations of SWCV, purple rectangle represents the CBV center at 500 hPa; **a2–a6** based on the conventional observed data; **b1–b6** based on the conventional plus intensive observed data). **a2** 0000 UTC 1 July; **a4** 1200 UTC 1 July; **a6** 0000 UTC 2 July; **b1** 1800 UTC 30 June; **b2** 0000 UTC 1 July; **b3** 0600 UTC 1 July; **b4** 1200 UTC 1 July; **b5** 1800 UTC 1 July; **b6** 0000 UTC 2 July

due to lack of the intensive sounding observation in Jiange. At the vorticity field with the conventional plus intensive observed data (Fig. 10e), it could be seen that SWCV at 700 hPa exhibited strong and deep positive vorticity in the upper-middle-lower troposphere (1000–250 hPa) with the center at 500 hPa in 30.5°N because of its development. TPV at 500 hPa was located at the positive vorticity area between surface and 400 hPa, and its range and strength of the positive vorticity were much smaller than SWCV. And there was a positive vorticity center from 850 to 700 hPa in Gansu. Due to the lack of the intensive sounding observation in Jiange, the conventional observed data (Fig. 10b) showed that the positive vorticity center of SWCV was much lower at 850 hPa and more south in 29.5°N, and the positive vorticity scope of TPV was larger. At the temperature deviation field with the conventional plus intensive observed data (Fig. 10f), near SWCV, there was a wide and deep northward-slantwise warm zone between 26°N and 32°N from surface to 150 hPa, which connects with the warm centers at 100 hPa over Gansu and at surface over Yunnan–Guizhou Plateau, respectively. SWCV at 700 hPa was located in the warm zone with a warm center, and there was a large warm center at 300 hPa over it. And the upper warm center should be associated with the condensation latent heat release. Furthermore, the ascending motion well corresponds with the warm air area. TPV at 500 hPa was located in the cold area with  $< -3$  °C cold center below it and warm area above it. Due to the lack of the intensive sounding observation in Jiange, the conventional observed data (Fig. 10c) show that the range of cold center below TPV and other warm centers was larger.

## 5.2 Vertical structure during merging and movement southward

At 0600 UTC 30 June, SWCV and TPV met, coupled, and formed a new vortex CBV. From the vertical distributions along 105°E from 23°N to 38°N, during the two vortices' merging, at the divergence field with the intensive observed data (Fig. 11a), it shows that below 500 hPa, the convergence centers of SWCV and TPV extended toward the north and the south, respectively, and combined with each

other at 31.5°N. The convergence area covered from 26°N to 35°N, and there was a convergence tongue up to 400 hPa near CBV. Above 500 hPa, the 200 hPa divergence center weakened and the 250 hPa convergence center vanished before merging (Fig. 10d), and it became a divergence area with one center over CBV and another center in the north of CBV. Especially, the ascending motion obviously strengthened in the range and the intensity, which controls Sichuan Basin, southern Gansu, and Yunnan–Guizhou Plateau from surface to 150 hPa, accompanied by a vertical circulation cell in cyclone from 23°N to 29°N with the convergence center at 250 hPa. At the vorticity field with the intensive observed data (Fig. 11b), because of the merging, the positive vorticity of CBV increased quickly and widely compared with that before merging (Fig. 10e), especially its range and intensity. The positive vorticity extended up to 150 hPa and the large vorticity center located at the south of CBV was more deep from 850 to 400 hPa, which well corresponds with heavy rainfall area. And it seems TPV was merged to SWCV, and CBV was very similar to SWCV in vorticity. At the temperature deviation field with the intensive observed data (Fig. 11c), CBV exhibited a cold-core vortex with deep cold air, and a strong cold air drop existed between 925 and 500 hPa with a center at 850 hPa. And the warm area and its center in SWCV before merging (Fig. 10f) weakened and shrank back to the south. And it seems SWCV was merged to TPV and CBV was very similar to TPV in temperature. In fact, the cold center below TPV moved down along the side slope of northern Sichuan Basin to 31.5°N and it continued to strengthen and grow with an upward cold tongue due to the merging, the temperature deviation of it was  $< -5$  °C, and rainfall mainly distributed in the ascending motion area at the front of CBV.

Here, from the vertical distributions along 32°N from 98°E to 113°E with the intensive observed data (Figures omitted), it can be further obtained that during the two vortices' merging, at the divergence field, there were a convergence area from surface to 700 hPa, a narrow divergence area at 600 hPa, and a strong convergence zone over 400 hPa and a strong divergence area at 150 hPa in Sichuan Basin (103.5°E–107.5°E). With the low troposphere occupied by convergence area, the configuration of low-level convergence and high-level divergence generated strong ascending motion. Rainfall area was located in the ascending motion area in central Sichuan Basin (105°E–106°E). At the vorticity field, the vorticity center of CBV was located at 500 hPa with  $3 \times 10^{-5} \text{ s}^{-1}$ , but its influence range was small. At the temperature deviation field with the intensive observed data (Fig. 11d), CBV at 500 hPa was located at the cold area from surface to 150 hPa, and below CBV, there existed the strong cold-air drop which leaned from the side slope of western Sichuan

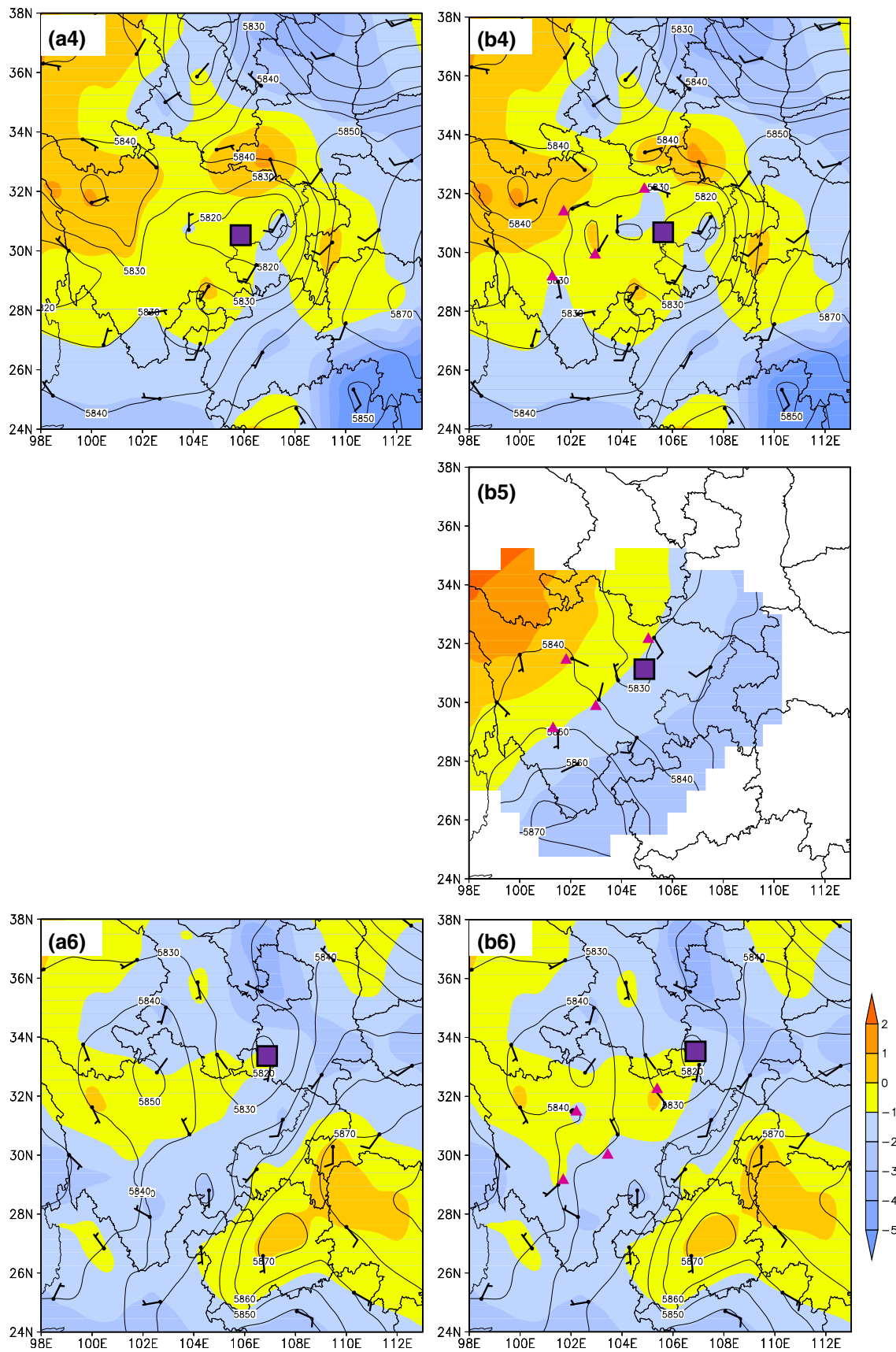
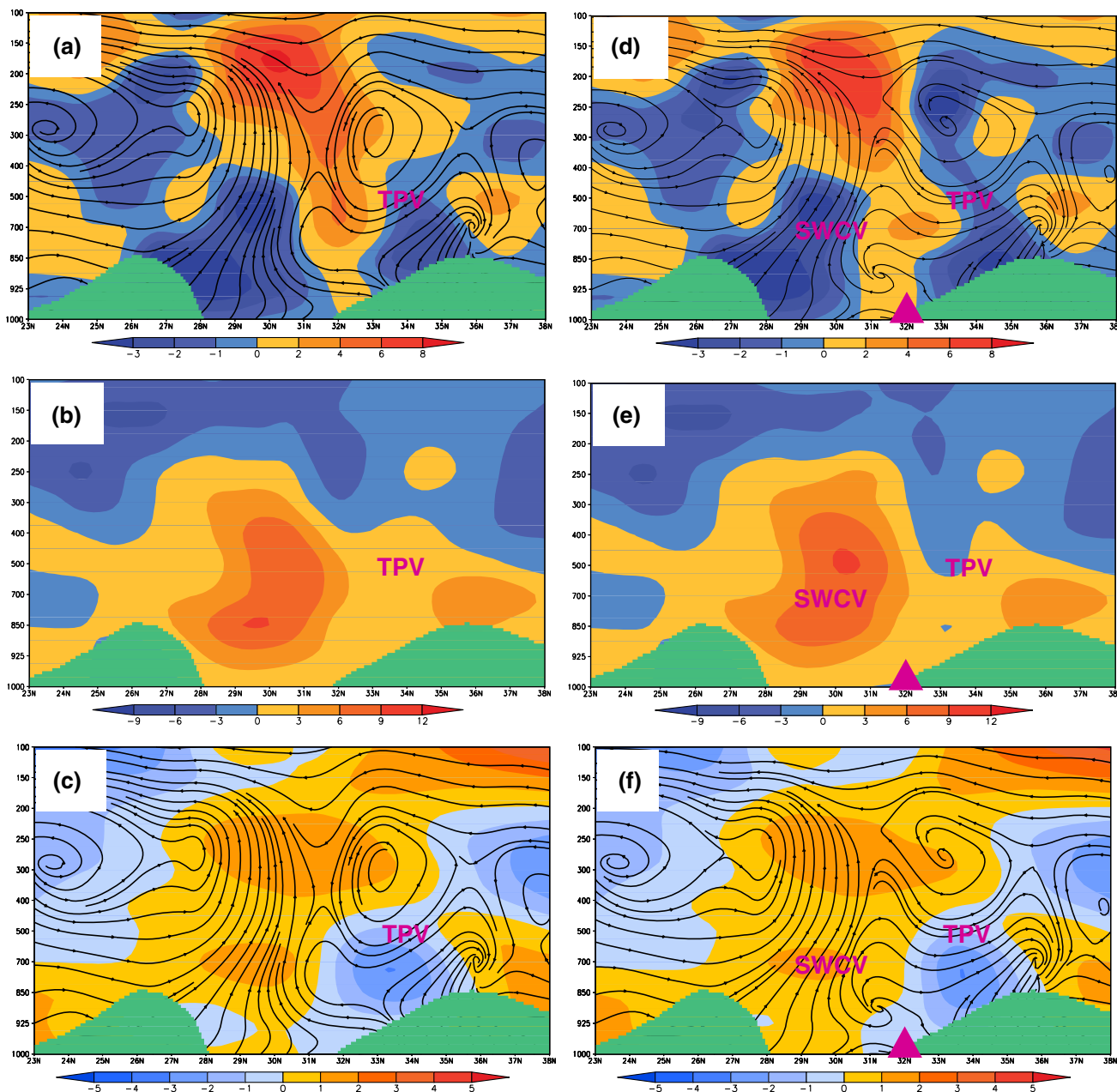


Fig. 9 continued



**Fig. 10** The vertical distributions of divergence, vorticity, temperature deviation, and flow field from 23°N to 38°N along 105°E at 0000 UTC 30 June (green shadows represent terrain, SWCV and TPV represent its latitude position, respectively, triangle represents the

location of Jiange; **a–c** based on the conventional observed data; **d–f** based on the conventional plus intensive observed data). **a, d** divergence (unit:  $10^{-5} \text{ s}^{-1}$ ) and flow field; **b, e** vorticity (unit:  $10^{-5} \text{ s}^{-1}$ ); **c, f** average temperature deviation (unit:  $^{\circ}\text{C}$ ) and flow field

Basin to the interior. There was one deep warm air from 700 to 150 hPa in western Sichuan plateau flowing eastward and another warm air between surface and 700 hPa on the east of Sichuan Basin flowing westward into Sichuan Basin. The easterly passed the cold-air drop to climb along the side slope of western Sichuan plateau and joined with the westerly over western Sichuan plateau, which became a slantwise upward flow. So, a distinct confluence area of warm air-cold air and a dense temperature deviation gradient area appeared. The flow moved

upward to cold areas along the temperature deviation gradient, similar to the interface of front, and the above area well corresponds with heavy rainfall. However, there is no conventional observation at 0600 UTC.

At 1200 UTC 30 June, CBV moved southward to near Chengdu. At the divergence field with the conventional plus intensive observed data (Fig. 12d), it can be seen that CBV was divergence area from surface to 150 hPa with the divergence center around 700 hPa, and there were widely downward flow above 700 hPa and easterly flow below

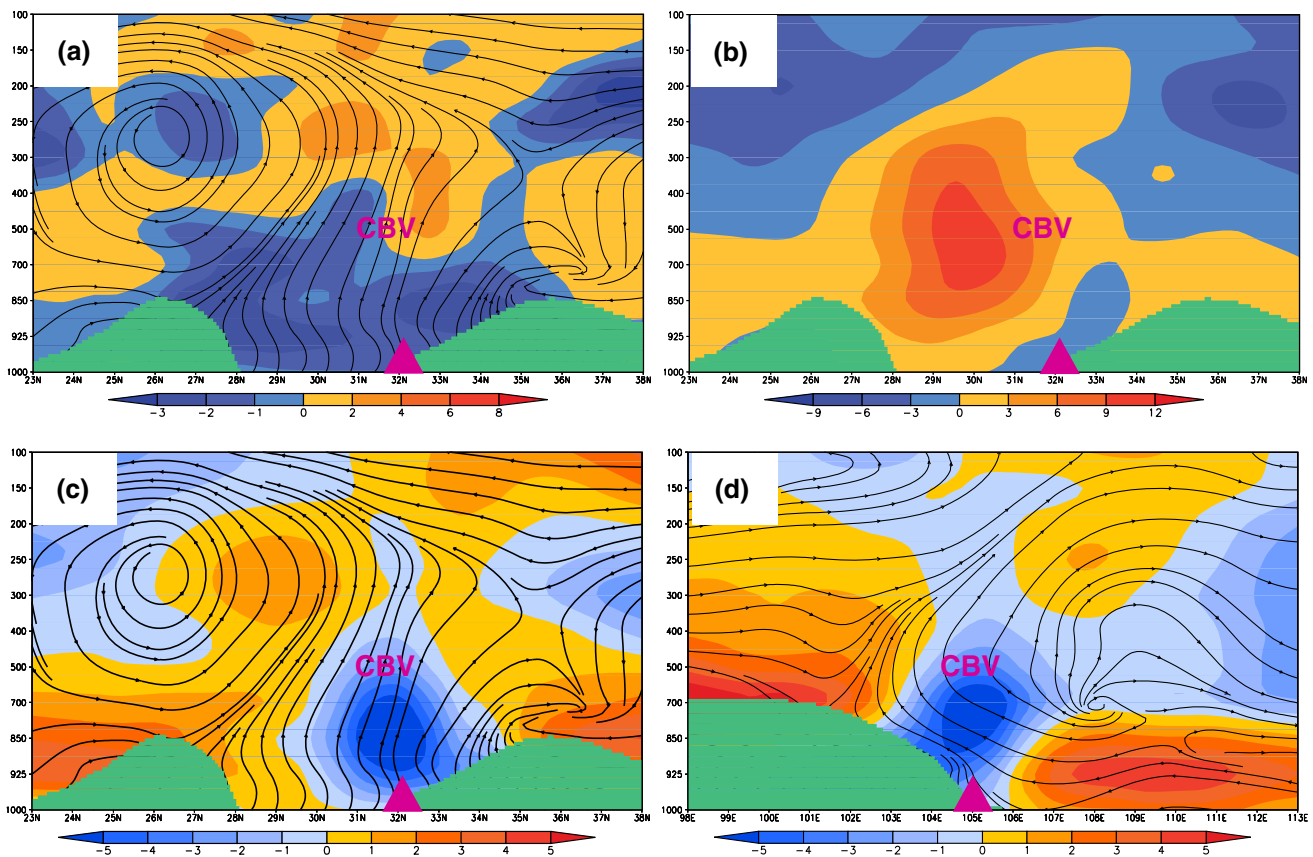


**Fig. 11** The vertical distribution of divergence, vorticity, temperature deviation, and flow field at 0600 UTC 30 June with the intensive observed data (*green shadows* represent terrain, CBV presents its position, *triangle* represents the location of Jiange). **a** divergence

(unit:  $10^{-5} \text{ s}^{-1}$ ) and flow field; **b** vorticity (unit:  $10^{-5} \text{ s}^{-1}$ ); **c** average temperature deviation (unit:  $^{\circ}\text{C}$ ) and flow field; **d** average temperature deviation (unit:  $^{\circ}\text{C}$ ) and flow field. **a–c** From  $23^{\circ}\text{N}$  to  $38^{\circ}\text{N}$  along  $105^{\circ}\text{E}$ ; **d** from  $98^{\circ}\text{E}$  to  $113^{\circ}\text{E}$  along  $32^{\circ}\text{N}$

700 hPa from  $101^{\circ}\text{E}$  to  $106^{\circ}\text{E}$ , which is consistent with Huang and Li (2007). At the same time, at the east side of CBV ( $106^{\circ}\text{E}$ – $108^{\circ}\text{E}$ ) existed a deep convergence area and significant ascending motion between surface and 250 hPa, which is conducive to CBV movement eastward. The strong convergence area at the west side of CBV ( $100^{\circ}\text{E}$ – $103^{\circ}\text{E}$ ) at upper level and the sinking motion were against the low system occurrence at the side slope of western Sichuan plateau. However, the conventional observed data (Fig. 12a) show there was no strong divergence center below CBV, and the ascending motion at the east side of CBV was relatively weaker. And the west side of it appeared a unreal intense ascending motion with convergence at lower level and divergence at upper level. At the vorticity field with the conventional plus intensive observed data (Fig. 12e), the positive vorticity area of CBV extended from surface up to 200 hPa and developed much deeply. The maximum center was located in the middle troposphere with  $9 \times 10^{-5} \text{ s}^{-1}$ . It is important to note that the vertical structure of positive vorticity of CBV had the eastward-slantwise feature, which may indicate the eastward movement next. Although Fig. 12b with the conventional

observed data is similar to the Fig. 12e, the range of positive vorticity center was relatively larger, and cannot reflect the eastward-slantwise feature of CBV vorticity structure. At the temperature deviation field with the conventional plus intensive observed data (Fig. 12f), BCV at 500 hPa was a cold center with the structure of lower-part cold and upper-part warm. But the cold center of CBV obviously weakened with temperature deviation gradient reducing at its east side, and rainfall was still located at the ascending motion area where cold air and warm air conflated with each other. However, the conventional observed data (Fig. 12c) show that the temperature deviation gradient at the east side of CBV ( $106^{\circ}\text{E}$ – $108^{\circ}\text{E}$ ) was much weaker.

### 5.3 Vertical structure during movement eastward

Seen from  $98^{\circ}\text{E}$  to  $113^{\circ}\text{E}$  along  $31^{\circ}\text{N}$ , at 0000 UTC 1 July, CBV moved eastward to eastern Sichuan. At the divergence field with the conventional plus intensive observed data (figures omitted), it could be identified that CBV at 500 hPa exhibited convergence with the upper level divergence. And there existed a deep convergence column



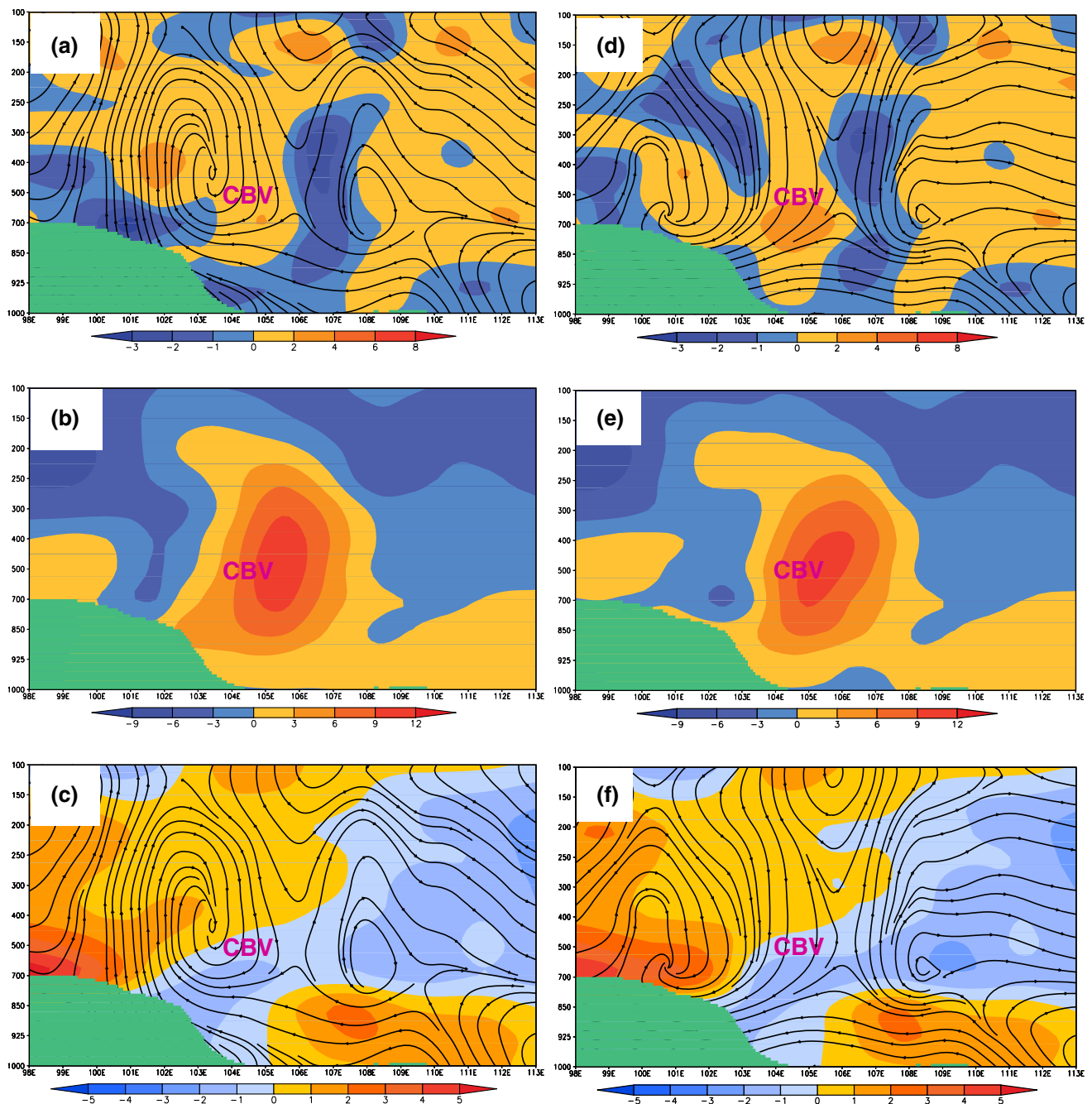


**Fig. 12** The vertical distributions of divergence, vorticity, temperature deviation, and flow field from 98°E to 113°E along 31°N at 1200 UTC 30 June (*green shadows* represent terrain, CBV presents its longitude position; **a–c** based on the conventional observed data;

**d–f** based on the conventional plus intensive observed data). **a, d** Divergence (unit:  $10^{-5} \text{ s}^{-1}$ ) and flow field; **b, e** vorticity (unit:  $10^{-5} \text{ s}^{-1}$ ); **c, f** average temperature deviation (unit: °C) from 98°E to 113°E and flow field

from surface to 150 hPa with upper level center and lower level center at the east part of CBV, and there was a convergence area from 850 to 250 hPa with a center at 700 hPa at the side slope of western Sichuan Basin. These areas around CBV were corresponding to the ascending motion. There was a divergence center at 500 hPa with upper level convergence center over northeastern Chongqing and western Sichuan plateau, respectively. At

the same time, these areas appeared downward flow at 98°E–101°E and 109°E–112°E, which formed two secondary circulation cells in the vertical direction with the ascending motion at 102°E–108°E. But the conventional observed data only show that CBV at 500 hPa was divergence area with a strong divergence center over it. At the vorticity field with the conventional plus intensive observed data (figures omitted), the positive vorticity of

CBV strengthened from surface up to 150 hPa with the  $>12 \times 10^{-5} \text{ s}^{-1}$  center at 500 hPa. However, the conventional observed data show that the intensity and range of the positive vorticity were relatively smaller. At the temperature deviation field with the conventional plus intensive observed data (figures omitted), CBV at 500 hPa remained the structure of lower-part cold and upper-part warm, and the confluence of cold air and warm air still existed. But its cold center basically disappeared, the temperature deviation gradient further reduced. And the conventional observed data show that the range of warm air was a little smaller.

At 1200 UTC 1 July, CBV stayed in eastern Sichuan. At the divergence field with the conventional plus intensive observed data (figures omitted), it shows that CBV was in the divergence center (106°E–107°E) at 500 hPa with a strong convergence center at 250 hPa and a convergence center at 850 hPa. So, the ascending motion around CBV was inhibited significantly and weakened, resulting in a strong downward flow between 700 and 200 hPa and easterly flow below 700 hPa. And there appeared the structure of 200 hPa convergence, 300 hPa divergence, and 700 hPa convergence at the side slope of western Sichuan plateau. The conventional observed data show that the 500 hPa divergence center of CBV was much smaller and sinking motion was weaker. And the 700 hPa convergence center did not appear at the side slope of western Sichuan plateau. At the vorticity field with the conventional plus intensive observed data (figures omitted), with CBV attenuation, the vorticity center of it weakened and the positive vorticity area dropped to under 250 hPa, especially, the strong vorticity center was located in the western CBV. The conventional observed data show that the range of positive vorticity center was relatively smaller. At the temperature deviation field with the conventional plus intensive observed data (figures omitted), with the cold air entering into Sichuan Basin around 700 hPa from the east, the lower level warm air weakened rapidly and retreated eastward gradually, the temperature deviation in CBV dropped very much and rainfall also decreased. But, the conventional observed data did not well reflect the cold air invading process toward Sichuan Basin.

## 6 Frontogenetical process of CBV

Figure 11 shows that the formation of CBV had obviously frontogenetical feature. Below, the frontogenetical function is used to analyze the early evolution of CBV. The frontogenesis expression (Wu 1999) was

$$F_h = \frac{d}{dt} |\nabla_h \theta| = T_1 + T_2 + T_3 + T_4 \quad (1)$$

$$T_1 = \left( \frac{\partial \theta}{\partial x} \frac{\partial Q}{\partial x} + \frac{\partial \theta}{\partial y} \frac{\partial Q}{\partial y} \right) / |\nabla_h \theta| \quad (2)$$

$$T_2 = - \left( \frac{\partial \omega}{\partial x} \frac{\partial \theta}{\partial x} + \frac{\partial \omega}{\partial y} \frac{\partial \theta}{\partial y} \right) \frac{\partial \theta}{\partial z} / |\nabla_h \theta| \quad (3)$$

$$T_3 = - \frac{D}{2} / |\nabla_h \theta| \quad (4)$$

$$T_4 = - \frac{1}{2} \left[ E_{st} \left( \frac{\partial \theta}{\partial x} \right)^2 + 2E_{sh} \left( \frac{\partial \theta}{\partial x} \right) \left( \frac{\partial \theta}{\partial y} \right) - E_{st} \left( \frac{\partial \theta}{\partial y} \right)^2 \right] / |\nabla_h \theta| \quad (5)$$

$$Q = \frac{d\theta}{dt} \quad (6)$$

$$E_{st} = \frac{\partial u}{\partial x} - \frac{\partial v}{\partial y} \quad (7)$$

$$E_{sh} = \frac{\partial v}{\partial x} + \frac{\partial u}{\partial y} \quad (8)$$

$$\zeta = \frac{\partial v}{\partial x} - \frac{\partial u}{\partial y} \quad (9)$$

$$D = \frac{\partial u}{\partial x} + \frac{\partial v}{\partial y} \quad (10)$$

$T_1$ ,  $T_2$ ,  $T_3$ , and  $T_4$  represent adiabatic heating item, vertical motion item, horizontal convergence item, and horizontal deformation item, respectively. However, due to the data limitation, estimation of vertical velocity and adiabatic heating in real atmosphere is difficult, and thus the horizontal convergence item  $T_3$  is chosen to analyze the frontogenetical process of CBV. It showed that during the formation of CBV, there were very obvious frontogenetical characteristics.

Before two vortices' merging at 0000 UTC 30 June (Fig. 13a), there was a weak frontogenetical area ( $F_n > 4 \times 10^{-10} \text{ K s}^{-1} \text{ m}^{-1}$ ) at 850 hPa at the border of Sichuan and Chongqing. When two vortices couple at 0600 UTC 30 June (Fig. 13b), there were very strong frontogenesis over Sichuan Basin, and a huge frontogenetical center appeared at the central Sichuan Basin where the positive  $F_n$  reached  $14 \times 10^{-10} \text{ K s}^{-1} \text{ m}^{-1}$  and CBV formed. After two vortices' merging at 1200 UTC 30 June (Fig. 13c), CBV weakened and the positive frontogenetical area broke into two centers located in northeastern Sichuan and southeastern Sichuan, respectively.

From the vertical distributions along 106°E, before two vortices' merging at 0000 UTC 30 June (Fig. 14a), a positive frontogenetical area arose at lower troposphere from 28°N to 35°N, which was located from the side slope of northern Sichuan Basin to Sichuan Basin. And one frontogenetical center appeared at 850 hPa below SWCV and another strong frontolysis center existed at 700 hPa blow TPV. At 800 hPa, there was a frontogenetical gradient area near 34°N, which presented a strong baroclinicity. When two vortices couple at

0600 UTC 30 June (Fig. 14b), there existed an obvious frontogenetical process between 29°N and 34°N. A large frontogenetical gradient area formed and spread downward to the lower troposphere. And the positive frontogenetical area strengthened and developed upward with the vertical structure of the south-positive and north-negative from 850 to 400 hPa at the coupling area near 31.5°N. This was advantageous to enhance the two vortices into one vortex CBV. After two vortices' merging at 1200 UTC 30 June (Fig. 14c), the positive frontogenesis center at lower troposphere weakened with CBV movement southward and CBV also gradually attenuated.

## 7 Vertical distribution of potential vorticity for the merging process

In order to analyze the merging process of two vortices, the potential vorticity (PV) (Ertel 1942) was adopted. The mathematical expression was

$$P = \alpha \zeta_{\sigma} \cdot \nabla \theta \quad (11)$$

Figure 15 shows the evolutions of PV along the vortices' center. Before the two vortices merged at 0000 UTC 30 June (Fig. 15a), TPV was in the positive PV area with 1PVU and moved southward. And SWCV was also in the positive PV area with 1.2PVU and moved northeastward. But there was a strong positive PV area from 700 to 300 hPa with the 1.8PVU center at 500 hPa, which was just located at the front of TPV and over SWCV. According to the conservation of PV, positive PV anomalies at the upper level always led to the development of cyclone at the lower level. So the enhanced PV near 31°N at 500 hPa promoted SWCV to develop rapidly. When the two vortices merge at 0600 UTC 30 June (Fig. 15b), TPV and SWCV merged and strengthened. Near 105°E, 31.8°N, two PV anomalies at lower level and upper level coupled with the maximum PV center of 2PVU at 450 hPa and the positive PV area developed and became larger from 900 to 250 hPa and from 27°N to 34°N, forming CBV. And the maximum center of positive PV was on the south of CBV, which indicates CBV will move southward. After the two vortices merged, CBV moved southward with the positive PV center. At 1200 UTC 30 June (Fig. 15c), CBV at 500 hPa was located at the 105°E and the maximum center of positive PV was on the east of CBV. So, CBV turned to move eastward and varied gradually with the positive PV center.

## 8 Effect of warm and moist air on rainfall

The occurrence of rainfall is closely related to warm and moist air, so pseudo-equivalent potential temperature is an important physical quantity to characterize atmospheric

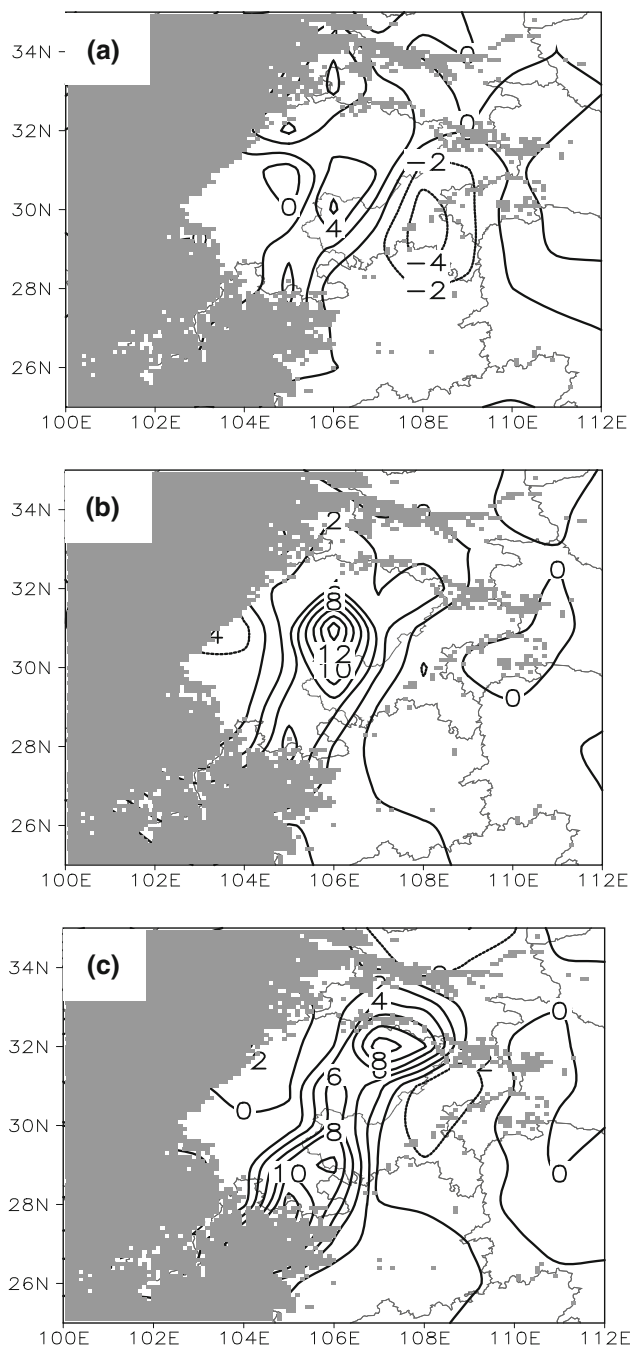


**Fig. 13** The distribution of the horizontal convergence item  $T_3$  of frontogenesis (contour, unit:  $10^{-10} \text{ K s}^{-1} \text{ m}^{-1}$ ; shading shows topography more than 1500 m) at 850 hPa on 30 June, **a** 0000 UTC; **b** 0600 UTC; **c** 1200 UTC

temperature and moisture. Figure 16 shows the distributions of pseudo-equivalent potential temperature  $\theta_{se}$  during the rainfall process. Before the two vortices' merging at 1200 UTC 29 June (Fig. 16a), there were high  $\theta_{se}$  areas in southeastern Sichuan and at the border of Sichuan and Shanxi indicating warm and moist air accumulated in Sichuan Basin. At 1800 UTC 29 (Fig. 16b), cold air began

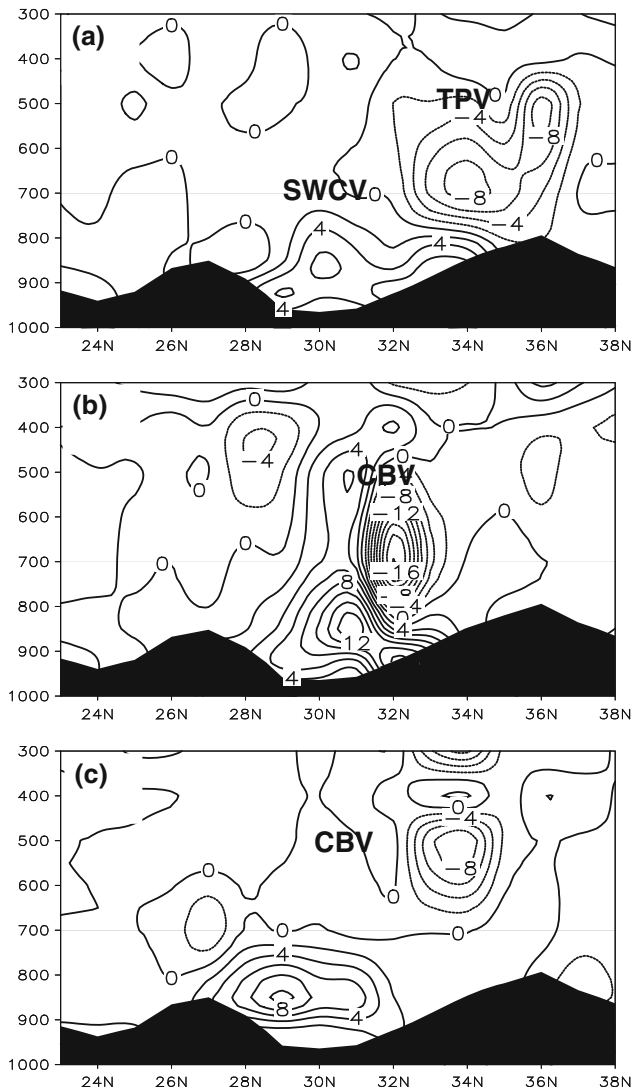


**Fig. 14** The vertical distribution of the horizontal convergence item  $T_3$  of frontogenesis (contour, unit:  $10^{-10} \text{ K s}^{-1} \text{ m}^{-1}$ ) from  $23^\circ\text{N}$  to  $38^\circ\text{N}$  along  $106^\circ\text{E}$  on 30 June (shading shadows represent terrain), **a** 0000 UTC; **b** 0600 UTC; **c** 1200 UTC

to invade into northern Sichuan gradually and the  $\theta_{se} < 354 \text{ K}$  area occupied northern Sichuan. At 0000 UTC 30 (Fig. 16c), SWCV moved northeastward further, and warm and moist air from the southwest influenced the borders of Chongqing, Guizhou and Sichuan with a  $360 \text{ K}$   $\theta_{se}$  tongue from the south. And under the influence of the returning cold air from northern China, a low  $\theta_{se}$  tongue from the north entered the margin of northeastern Sichuan. When the two vortices' merging at 0600 UTC 30 (Fig. 16d), TPV and SWCV met near  $32^\circ\text{N}$ , merged, and strengthened into CBV in northwestern Sichuan Basin. CBV formed a strong cold-core structure with the  $\theta_{se} < 327 \text{ K}$  center. Because of the confluences of cold air and warm air, heavy rainfall occurred in eastern Sichuan. After the two vortices' merging, CBV moved southward to

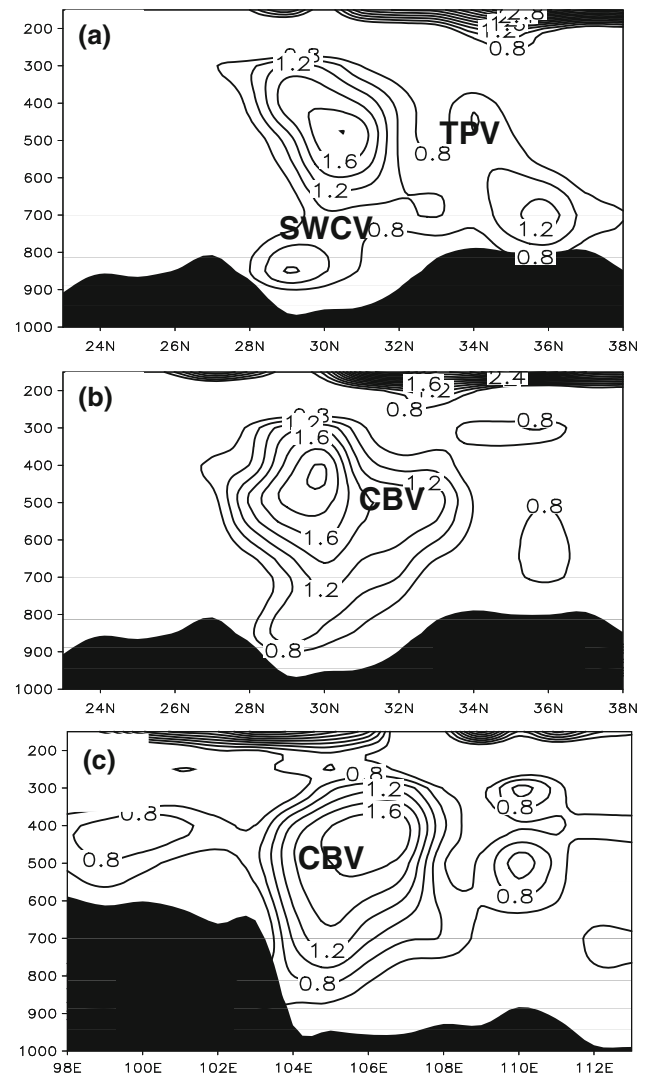


**Fig. 15** The distribution of potential vorticity (contour, unit: PVU) in the vertical meridional cross-section along the vortices' center from 0000 UTC 30 to 1200 UTC 30 June (shading shadows represent terrain); **a** 0000 UTC 30 along the  $105^\circ\text{E}$  vertical cross-section; **b** 0600 UTC 30 along the  $105^\circ\text{E}$  vertical cross-section; **c** 1200 UTC 30 along the  $31^\circ\text{N}$  vertical cross-section

near Chengdu in western Sichuan Basin at 1200 UTC 30 (Fig. 16e). The cold center of CBV weakened without low  $\theta_{se}$  center, but the warm and moist air continued to occupy northeastern Sichuan and Chongqing with the  $372 \text{ K}$   $\theta_{se}$  center, and CBV moved eastward and rainfall maintained in east-central Sichuan.

## 9 Conclusions

A rainstorm process caused by the interaction, especially the merging of TPV and SWCV, was analyzed in eastern Sichuan during 29 June–2 July 2013 based on the intensive

observation and the conventional observation. Some useful conclusions were drawn below:

1. During this rainstorm, the large-scale circulation was a large transverse trough maintained in Eurasia region. There existed the sustained westerly flow in northern China and a lot of short-wave troughs occurred on the north of Qinghai-Tibet Plateau and moved eastward to its downstream areas, which were conducive to TPV and SWCV movement. The warm and moist air from the Bay of Bengal and the South China Sea provided sufficient water vapor into Sichuan Basin. TPV at 500 hPa and SWCV at 700 hPa were the direct influence systems for the heavy rainfall weather.
2. Using the intensive observed data based on the conventional observed data, it could better reflect that SWCV originated in Muli on the south of Jiulong at the southeast of western Sichuan plateau and moved northeastward along Ya'an into Sichuan Basin, and TPV in the eastern Tibetan Plateau moved eastward on the north of western Sichuan plateau and then turned southward into Sichuan Basin. Especially, it could reveal the coupling process of TPV and SWCV, the evolutions of CBV in Sichuan Basin, and the resulting heavy rainfall. But only using the conventional observed data, the occurrences, movements and coupling process of SWCV and TPV, and its rainfall weather were not well reflected. And at the key period of the two vortices' coupling and CBV formation, there is no conventional observation at 0600 UTC 30 June. So, without the intensive observed data, it is very difficult to obtain accurate and clear understanding for the severe weather systems such as TPV and SWCV and its weather influences.
3. Combined with the intensive observed data at Jiulong, it could show that SWCV originated in warm area with the atmospheric heating over western Sichuan plateau. Due to the effect of warm air, SWCV developed and strengthened, but not moved out of the source area. When TPV advanced on the north of Sichuan Basin, after it occurred in the eastern Tibetan Plateau, the northerly flow at the west side of it made the easterly turn into northerly in Jiulong, and then SWCV left its source and moved to southern Ya'an. With cold air invading into the rear of SWCV, It strengthened again and moved out of western Sichuan plateau. The cold and dry air from the rear of TPV provided favorable condition for SWCV development and movement at lower level. And without the intensive observed data such as at Jinchuan, a large area of unreal vapor flux convergence existed in west-central Sichuan that was not consistent with local precipitation.
4. During the two vortices' coupling, TPV and SWCV exhibited some different contributions for the merged CBV in dynamic-thermodynamic property. Comparison showed that CBV was more close to SWCV in dynamic structure and TPV in thermodynamic structure. Especially, CBV had basically the same vorticity distribution with SWCV, and the same temperature distribution with TPV. But both TPV and SWCV had significant influences on the divergence distribution of CBV. And when CBV developed well, downward flow would appear at the center of it. These are important characteristics for the coupling process between TPV and SWCV.
5. Before CBV formation, TPV was in positive PV area and the positive PV at upper level motivated SWCV to strengthen at lower level. When the two vortices merged, the positive PV further developed both in the vertical direction and in the horizontal direction, and became larger and deeper with the stronger center of positive PV at upper level. But after the two vortices merged, the center of CBV did not coincide with the center of positive PV and the center of positive PV was generally located at the front of CBV. Furthermore, CBV will move toward the direction of the positive PV center. So, the center of positive PV can provide good indicative significance for the activities of vortex systems.
6. Before TPV and SWCV merged, there were not very obvious frontogenetical characteristics. When the two vortices merged, the process of frontogenesis developed rapidly around the center of CBV. A large frontogenetical gradient area formed from lower troposphere to upper troposphere. And it had the deep vertical structure of the south-positive and north-negative around the coupling area, where two vortices merged into a strong vortex CBV. Because TPV and SWCV come from the northwest and the southwest of Sichuan Basin, respectively, both had the different temperature-moisture property, and with their coupling each other, causing a large temperature deviation gradient area, it produced the frontal structure.
7. The confluence area of warm air and cold air with the high temperature deviation gradient corresponded well with rainfall weather. The strong cold air in CBV played an important role in the rainstorm process. During the strongest rainfall period, a low  $\theta_{se}$  center of 327 K appeared at CBV center. And the warm and moist areas at the east side of CBV exhibited high  $\theta_{se}$  distribution and heavy rainfall occurred in the large  $\theta_{se}$  gradient areas. The joint influences of Warm-moist air from the south and dry-cold air from the north are important conditions for this rainstorm in eastern Sichuan.



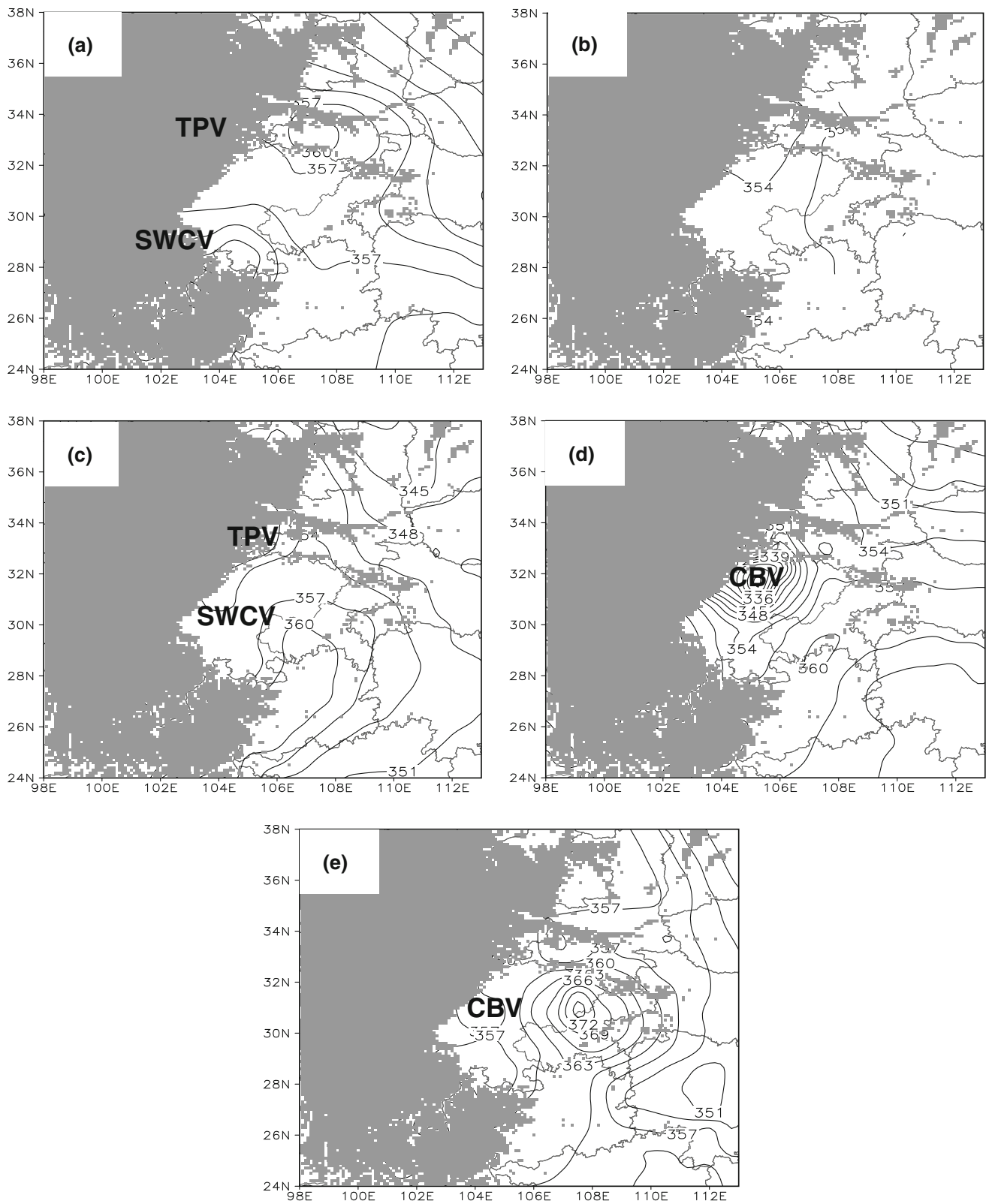


**Fig. 16** The pseudo-equivalent potential temperature  $\theta_{se}$  (K) from 1200 UTC 29 June to 1200 UTC 30 June with the conventional plus intensive observed data (*shading* shows topography more than

1500 m): **a** 1200 UTC 29 June; **b** 1800 UTC 29 June; **c** 0000 UTC 30 June; **d** 0600 UTC 30 June; **e** 1200 UTC 30 June

Finally, comparative analysis of the conventional observed data in the daily meteorological operation and the intensive observed data during the atmospheric scientific experiment indicated that the intensive observed data are much useful to reveal the generation and development of SWCV and TPV, as well as their effects on precipitation. Therefore, the special scientific experiment for the severe weather systems such as TPV and SWCV is very important for the research and application. It is necessary for meso- and small-scale weather to strengthen the intensive observation and field experiment during flood season in the future.

**Acknowledgments** The authors are very thankful to Dr. Michael L. Kaplan and the two anonymous reviewers whose constructive comments have improved the overall quality of the paper. This work was supported by the key project of the National Natural Science Foundation (No. 91337215), the National Natural Science Foundation of China (No. 41275051), the National Key Basic Research Development Program Project of China (No. 2012CB417202), and Special Fund for Meteorological Research in the Public Interest (GYHY201006053).

## References

- Chen S, Dell'osso L (1984) Numerical prediction of the heavy rainfall vortex over the eastern Asia monsoon region. *J Meteorol Soc Japan* 62:730–747
- Chen Z, Miao Q, Min WB (1998) Meso-scale structure analysis of a strong southwest China vortex. *J Appl Meteorol Sci* 9(3):273–282 (in Chinese)
- Chen Z, Min WB, Miao Q, He GB (2004) A case study of the coupling of southwest China vortex and Tibetan Plateau vortex. *Plateau Meteorol* 23(1):75–80 (in Chinese)
- Chen D, Li YQ, Huang RH (2007) Physical process of the southwest China vortex development and its effect on the rainfall in eastern Sichuan under the “saddle” pattern large-scale circulation background. *Chin J Atmos Sci* 31(2):185–201 (in Chinese)
- Ertel H (1942) Ein neuer hydrodynamische wirbelsatz. *Meteorol Z Braunschweig* 59:277–281
- Gu Q, Zhou CH, Qing Q, Zhang J (2008) A meso-scale analysis of a southwest China vortex rainstorm. *Meteorol Mon* 34(4):39–47 (in Chinese)
- Huang C, Li GP (2007) Two cases preliminary analysis of Tibetan Plateau vortex structure based on the satellite observation. *J Chengdu Univ Inf Technol* 22(4):253–259 (in Chinese)
- Lhasa Tibetan Project group of Qinghai-Tibetan Plateau meteorological research (1981) Research on the 500 hPa low vortex, wind shear on the Tibetan Plateau in summer. Science Press, Beijing (in Chinese)
- Li G (2007) Tibetan Plateau dynamic meteorology, 2nd edn. China Meteorological Press, Beijing (in Chinese)
- Li G, Liu HW (2006) An analysis of surface heat source forcing on the Tibetan Plateau Vortex. *J Trop Meteorol* 22(6):632–637 (in Chinese)
- Li Y, Zhao XB, Deng B (2010) Intensive observation scientific experiment of the southwest vortex in the summer of 2010. *Plateau Mt Meteorol Res* 30(4):80–84 (in Chinese)
- Li Y, Zhao XB, Zhang HL, Zhou CC (2011) Intensive observation scientific experiment of the southwest vortex in the summer of 2011. *Plateau Mt Meteorol Res* 31(4):7–11 (in Chinese)
- Li Y, Zhao XB, Zhang HL, Zhou CC (2012) Intensive observation scientific experiment of the southwest vortex in the summer of 2012. *Plateau Mt Meteorol Res* 32(4):1–8 (in Chinese)
- Liu F, Du WJ (1987) The formation and eastward movement of the Tibetan Plateau vortex inducing heavy rainfall in Sichuan Basin, the Tibetan Plateau effect on China weather in summer. China Meteorological Press, Beijing, pp 123–134 (in Chinese)
- Lu J (1986) Generality of the Southwest Vortex. China Meteorological Press, Beijing (in Chinese)
- Luo S (1992) Research on a few categories of synoptic system on the Tibetan Plateau and its adjacent areas. China Meteorological Press, Beijing (in Chinese)
- Luo S, Wei L (1985) Dynamic analysis of the Tibetan Plateau effects on a westerly trough cutting off on May 1979. *Plateau Meteorol* 3(1):19–29 (in Chinese)
- Miao Q (1999) A coupling interaction analysis of Tibetan Plateau synoptic system and the shallow synoptic system at leeward slope. *Sichuan Meteorol* 19(3):18–22 (in Chinese)
- O'Brien J (1970) Alternative solutions to the classical vertical velocity problem. *J Appl Meteorol* 9:197–203
- Shen R, Reiter ER, Bresch JF (1986) Numerical simulation of the development of vortices over the Qinghai-Xizang Plateau. *Meteorol Atmos Phys* 35:70–95
- Tao S, Ding Y (1981) Observational evidence of the influence of the Qinghai—Xizang (Tibet) Plateau on the occurrence of heavy rain and severe convective storms in China. *Bull Am Meteorol Soc* 62:23–30
- Wang B (1987) The development mechanism for Tibetan Plateau warm vortices. *J Atmos Sci* 44:2978–2994
- Wang B, Orlanski I (1987) Study of a heavy rain vortex formed over the eastern flank of the Tibetan Plateau. *Mon Weather Rev* 115:1370–1393
- Wang W, Ying-hwa K, Thomas TW (1993) A diabatically driven mesoscale vortex in the lee of the Tibetan Plateau. *Mon Weather Rev* 121:2542–2561
- Wu R (1999) Modern synoptic theory. Higher Education Press, Beijing (in Chinese)
- Wu G, Chen SJ (1985) The effect of mechanical forcing on the formation of a mesoscale vortex. *Q J R Meteorol Soc* 111:1049–1070
- Xiang S, Li YQ, Dian L, Yang S (2013) An analysis of heavy precipitation caused by a retracing plateau vortex based on TRMM data. *Meteorol Atmos Phys* 122:33–45
- Ye D, Gao YX (1979) Tibetan Plateau meteorology. Science Press, Beijing (in Chinese)
- Ying-Hwa K, Cheng LS, Bao JW (1988) Numerical simulation of the 1981 Sichuan flood. Part I: evolution of a mesoscale southwest vortex. *Mon Weather Rev* 116:2481–2504
- Zhang J, Zhu BZ (1988) Advances in Tibetan Plateau meteorology. Science Press, Beijing (in Chinese)
- Zhao Y, Wang YH (2010) A case analysis of the southwest China vortex rainstorm induced by Tibetan Plateau vortex. *Plateau Meteorol* 29(4):819–831 (in Chinese)